Hydrol. Earth Syst. Sci. Discuss., https://doi.org/10.5194/hess-2019-137
Manuscript under review for journal Hydrol. Earth Syst. Sci.
Discussion started: 18 April 2019

Hydrology and Earth System Sciences
Discussions

Influence of multi-decadal land use, irrigation practices and climate on riparian corridors across the Upper Missouri River Headwaters Basin, Montana

Melanie K. Vanderhoof[1], Jay R. Christensen[2], Laurie C. Alexander[3]

[1]US Geological Survey, Geosciences and Environmental Change Science Center, P.O. Box 25046, DFC, MS980, Denver, CO 80225, USA
[2]US Environmental Protection Agency, Office of Research and Development, National Exposure Research Laboratory, 26 W. Martin Luther King Dr., MS-642, Cincinnati, OH 45268, USA
[3]US Environmental Protection Agency, Office of Research and Development, National Center for Environmental Assessment, 1200 Pennsylvania Ave NW (8623-P), Washington, DC 20460, USA

Corresponding Author: Melanie K. Vanderhoof (mvanderhoof@usgs.gov, 303.236.1411)

Abstract

The Upper Missouri River Headwaters Basin (36,400 km^2) depends on its river corridors to support irrigated agriculture and world-class trout fisheries. We evaluated trends (1984-2016) in riparian wetness, an indicator of riparian condition, in peak irrigation months (June, July, August) for 158 km^2 of riparian area across the basin using the Landsat Normalized Difference Wetness Index (NDWI). We found that 8 of the 19 riparian reaches across the basin showed a significant drying trend over this period, including all three basin outlet reaches along the Jefferson, Madison and Gallatin Rivers. The influence of upstream climate was quantified using per reach random forest regressions. Although much of the interannual variability was explained by climate, especially by drought indices and annual precipitation, the significant drying trends persisted in the NDWI-climate model residuals, indicating that trends were not entirely attributable to climate. Over the same period we documented a 506% increase in center-pivot irrigation and an associated 39% decrease in non-center pivot irrigation basin-wide. Riparian reaches with a drying trend had a greater shift towards center-pivot irrigation relative to riparian reaches without such a trend (p<0.1). The drying trend, however, did not extend to river discharge. Over the same period, stream gages (n=7) showed a positive correlation with riparian wetness (p<0.05), but no trend in summer river discharge, suggesting that riparian areas may be more sensitive to changes in irrigation return flows, relative to river discharge. Identifying trends in riparian vegetation is a critical precursor to enhancing the resiliency of river systems and associated riparian corridors.

Hydrol. Earth Syst. Sci. Discuss., https://doi.org/10.5194/hess-2019-137
Manuscript under review for journal Hydrol. Earth Syst. Sci.
Discussion started: 18 April 2019

Hydrology and Earth System Sciences
Discussions

Keywords

Center-pivot, discharge, headwaters, Landsat, precipitation, wetness

1. Introduction

Riparian ecosystems provide critical biological, chemical and hydrological functions (Fritz et al., 2018). Defined as semi-terrestrial areas influenced by freshwaters at the interface of rivers and adjacent upland areas (Naiman et al., 2005), riparian ecosystems store water, nutrients, and sediments, reducing downstream flood impacts and non-point source pollution (Lowrance et al., 1984; Vivoni et al., 2006). They also provide corridors for biotic movement and migration, particularly through arid, urban and agricultural landscapes (Boutin and Belanger, 2003; Lees and Peres, 2008), and maintain fish habitat by lowering stream temperatures and contributing in-stream woody debris (Poole and Berman, 2001; Isaak et al., 2012). Long-term trends in the degradation of riparian areas are common globally (Stromberg, 2001; Richardson et al., 2007). The hydrological alteration of rivers, including dam construction, ditching, flow regulation, and pumping of surface and ground water for human use, can alter flow timing and magnitude leading to riparian degradation including changes to riparian functioning, loss of riparian extent, and shift in species composition (Poff et al., 1997; Nilsson and Berggren, 2000; Sweeney et al., 2004). Periodic drought and continued water withdrawals degrade cold-water spawning and rearing habitat for salmonid species (Clancy, 1988; Isaak et al., 2012). Balancing anthropogenic water needs while maintaining or enhancing riparian ecosystem integrity requires an improved understanding of the relationship between water extraction, river discharge, and riparian vegetation (Jones et al., 2010; Cunningham et al., 2011).

Irrigated agriculture is a primary consumptive use of water in the United States and globally. Across the United States, 26% of surface water withdrawals and 68% of groundwater withdrawals are attributable to agricultural irrigation (Dieter et al., 2018). Globally, irrigation accounts for 70% of water withdrawals (Wisser et al., 2008). Expansion of agricultural irrigation over the past centuries and shifts in irrigation methods over the past decades have led to major gains in agricultural productivity, food security, profitability, and crop diversification (Falkenmark and Lannerstad, 2005). As a primary use of water withdrawals and water consumption, however, irrigated agriculture can be expected to play a key role in local water cycles. When gravity-fed (i.e., flood) irrigation is applied, water that is not evaporated or

transpired by plants, replenishes soil water storage, recharges aquifers, and contributes return flows to streams and wetlands (Peterson and Ding, 2005; Perry, 2017; Grafton et al., 2018). Additional groundwater recharge also comes from unlined ditch systems used to convey water to agricultural fields. Return flow from excess irrigation has been argued to have artificially elevated autumn and winter streamflow for decades (Kendy and Bredehoeft, 2006). As farmers switch to more modern irrigation techniques, such as center pivot irrigation, they can achieve greater crop yields and gross revenue with less water, improving their "crop per drop" ratio (or water use efficiency; Peterson and Ding, 2005). This change, however, is also be expected to have hydrological consequences, namely increased evapotranspiration, and a reduction in surface runoff and subsurface recharge (Ward and Pulido-Velazquez, 2008; Grafton et al., 2018) which can impact local aquifers (Peterson and Ding, 2005; Pfeiffer and Lin, 2014), base flow (Kendy and Bredehoeft, 2006; Gosnell et al., 2007), as well as riparian ecosystems (Carrillo-Guerrero, 2013).

Although water withdrawals for irrigation may impact local water cycling, patterns in river discharge and riparian vegetation are largely driven by the watershed's climate patterns. Riparian vegetation tends to be adapted to highly variable fluvial disturbance regimes, a product of seasonal and interannual variability in river discharge, with riparian wetness peaking during episodic storm and flood events and lessening during drought events (Hughes, 2005; Goudie, 2006; Capon, 2013). River discharge and groundwater hydrology, in turn, tends to be highly responsive to variability in precipitation and evaporative demand (Goudie, 2006; Dragoni and Sukhiga, 2008; Hausner et al., 2018). Further, in snow-melt dominated systems, changes in snow pack storage and rain to snow event ratios can influence the timing of river discharge and regional groundwater recharge, impacting water availability in associated riparian areas (Rood et al., 2008).

While satellite imagery offers a cost-effective means to monitor landscapes, the narrow, linear nature of riparian corridors presents a challenge for ecosystem characterization with remote sensing tools (Klemas, 2014; Vanderhoof and Lane, 2019). Along large rivers, Landsat satellites provide a multi-decadal source of imagery to monitor changes in riparian vegetation (Jones et al., 2010; Henshaw et al., 2013). Remote sensing can also complement field data to enhance our understanding of the relationship between riparian vegetation and agents of change, such as climate (Huntington et al., 2016). The Normalized Difference Vegetation Index (NDVI)

(Tucker, 1979) is the most commonly used spectral index to evaluate changes in riparian vegetation over time (Fu and Burgher, 2015; Hamdan and Myint, 2015; Nguyen et al., 2015; Hausner et al., 2018). Trends in riparian greenness have been related successfully to climate variables and river discharge (Shafroth et al., 2002; Fu and Burgher, 2015; Nguyen et al., 2015), in part because riparian and wetland herbaceous species can respond rapidly to changes in soil moisture. Thus, riparian greenness tends to reflect river corridor hydrologic processes (Stromberg et al., 2001, 2006; Jones et al., 2008). Other indices can also potentially inform riparian wetness. For instance, the normalized difference wetness index (NDWI) was designed to be sensitive to changes in leaf and soil water content as well as to identify waters associated with wetlands or floodplains (Gao, 1996; McFeeters, 1996). This index has been used successfully, for example, to monitor changes in the extent of waterlogged areas (e.g., Chatterjee et al., 2005; Chowdary et al., 2008).

Despite the potential for satellite imagery to characterize plant-water interactions along riparian corridors, few studies have evaluated the impact of changing irrigation methods on riparian vegetation (Klemas, 2014; Perry, 2017), or have attempted to distinguish the relative influence of climate and agricultural irrigation on riparian vegetation. The Upper Missouri River Headwaters (UMH) Basin in southwestern Montana provides an excellent case study for exploring the interactions between climate, irrigation and riparian vegetation. The basin contains the Jefferson, Madison, and Gallatin Rivers, all of which support world-class cold-water trout fisheries that provide substantial economic value to the region (Duffield et al., 1992; Kerkvliet et al., 2002; Gosnell et al., 2007). In addition, the agricultural valleys of the basin are very productive yet rely on a complex irrigation system to water crops grown in and near riparian areas. Irrigation accounts for 97% of Montana's consumptive water use (Clifford, 1995; Dieter et al., 2018). Along with the high demand for irrigation water (Goklany, 2002; Schaible and Aillery, 2012), there are also increasing public water supply needs in the basin (Hansen et al., 2002; Gude et al., 2006). In addition, the timing of peak river flows is predicted to change, attributable to warmer temperatures at higher elevations and more precipitation in winter and early spring occurring as rainfall rather than snow (Pederson et al., 2011, 2013; USBR, 2012). All of these factors are contributing to an increasingly uncertain supply of water across the basin, particularly in the late summer. This uncertainty, in turn, has elevated interest in improving the resiliency of local streams and rivers so that the basin can continue to support the agricultural,

recreational, municipal and ecological needs of the watershed (Ziemer et al., 2006; Jones et al., 2012; Gärtner et al., 2013). In this study we used a time series of Landsat imagery (1984-2016) together with climate datasets, agricultural datasets, and U.S. Geological Survey (USGS) stream gage datasets to explore trends over time in riparian vegetation for the major river valleys across the UMH Basin. We sought to link the temporal trends not explained by climate to changes in land use type and intensity. Our research questions included:

1. How does remotely sensed riparian wetness across the UMH Basin reflect interannual variability in climate and river discharge?
2. How and to what degree are trends in riparian wetness from 1984-2016 attributable to changes in climate versus shifts in land use such as irrigation practice?

2. Methods

2.1 Study Area

The study area was the UMH Basin (36,400 km^2). Near the basin outlet, the Jefferson, Madison ,and Gallatin Rivers merge to form the Missouri River at Three Forks, Montana. A total of nine rivers were included in the analysis with riparian vegetation divided into 19 riparian reaches (Fig. 1). Hydrologic regimes of the rivers across the basin are snow-melt dominated (Markstrom et al., 2016; Cross et al., 2017) with multiple mountain ranges contributing surface runoff and ground water recharge to valley aquifers (Hackett et al. 1960; Slagle 1995). Annual precipitation across the basin averages 565 mm yr^{-1}, most of which falls in the mountains, where it is received primarily as snow (Fig. 2). The annual maximum and minimum temperatures average 10 °C and −3 °C respectively (1981-2010 period of record) (PRISM Climate Group, 2018). Elevations across the basin range from 1231 m to 3433 m (Gesch, 2002). While the mountain ranges are dominated by evergreen forest (35%), at lower elevations, the forest gives way to herbaceous vegetation (35%) and shrub/scrub (20%) cover types that dominate the large river valleys (Homer et al., 2015, Fig. 2). Agriculture occurs primarily in the lower elevations adjacent to many of the major rivers. As of 2017, alfalfa was the most common crop (41%), followed by other non-alfalfa hay crops (25%), barley (11%) and spring wheat (11%) (USDA, 2018). The riparian ecosystems along the major rivers are dominated by tree species including cottonwood (*Populus* spp.), willow (*Salix* spp.), and alder (*Alnus* spp.); shrubs including chokecherry (*Prunus virginiana*), snowberry (*Symphoricarpos* spp.), and wild rose (*Rosa*

Hydrol. Earth Syst. Sci. Discuss., https://doi.org/10.5194/hess-2019-137
Manuscript under review for journal Hydrol. Earth Syst. Sci.
Discussion started: 18 April 2019

Hydrology and Earth System Sciences
Discussions

woodsia); and wet meadows dominated by cattails (*Typha* spp.), sedges (*Carex* spp.), and rushes (*Juncus* spp.). Warming temperatures in March and April initiate snowmelt and a corresponding increase in river discharge. Spring precipitation and snowmelt produce peak river discharge in May and June (Cross et al., 2017) followed by a sharp decline in July and August due to a dwindling supply of melt water from snow pack and consumptive use from withdrawals. Late autumn through early spring are generally characterized by lower flow conditions, presumably dominated by baseflow contributions from groundwater discharge (Cross et al., 2017). Major waterbodies across the basin are predominately reservoirs located upstream from dams (Fig. 1b) that support irrigation, hydropower, and recreation.

Hydrol. Earth Syst. Sci. Discuss., https://doi.org/10.5194/hess-2019-137
Manuscript under review for journal Hydrol. Earth Syst. Sci.
Discussion started: 18 April 2019

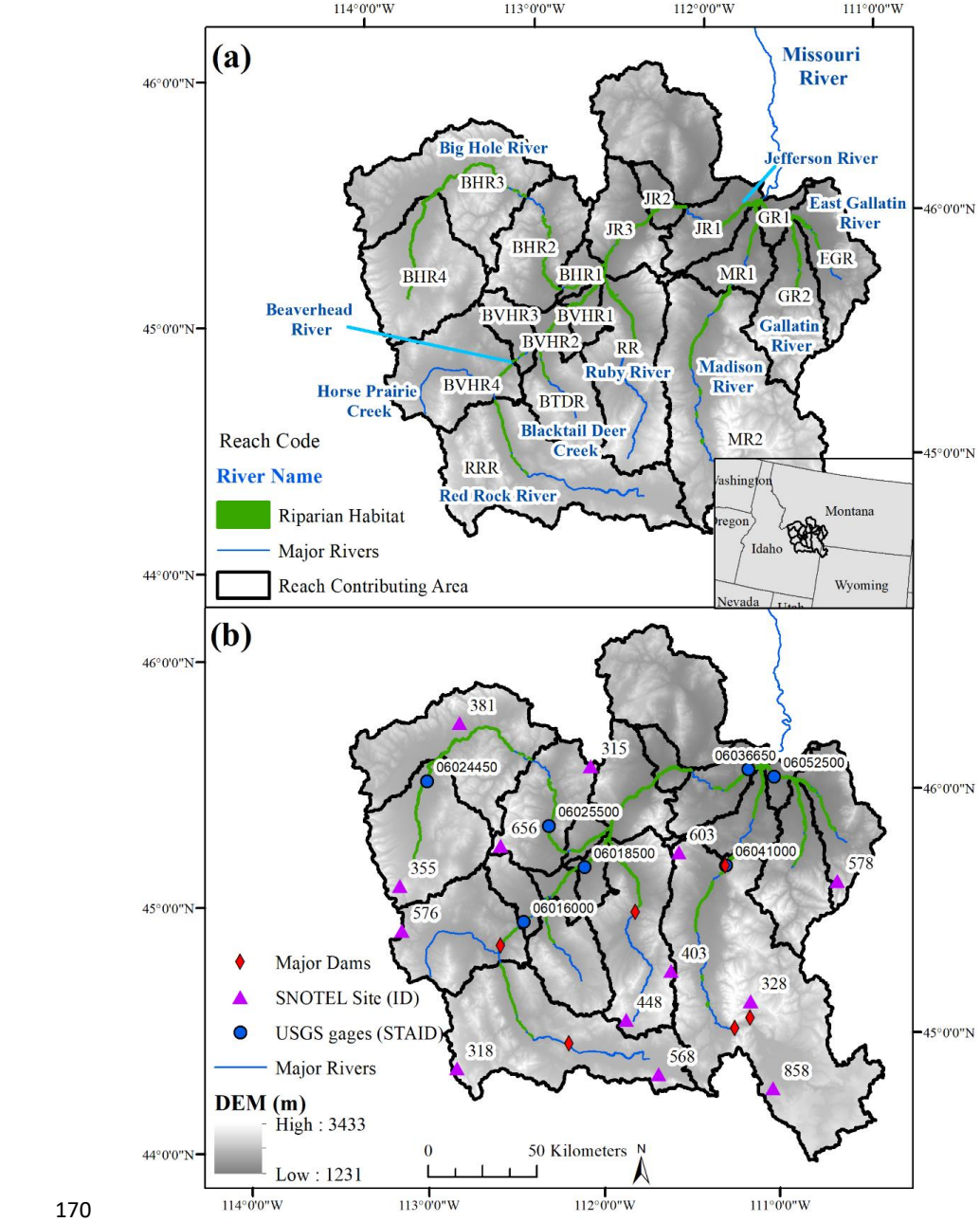

Figure 1. (a) The major rivers considered in the analysis, the distribution of the riparian areas evaluated, and the division of the riparian areas into reaches across the Upper Missouri River Headwaters Basin, southwestern Montana, USA. (b) The spatial distribution of the U.S. Geological Survey stream gages and snow telemetry (SNOTEL) sites considered in the analysis. STAID: Station ID, DEM: Digital Elevation Model.

Hydrol. Earth Syst. Sci. Discuss., https://doi.org/10.5194/hess-2019-137
Manuscript under review for journal Hydrol. Earth Syst. Sci.
Discussion started: 18 April 2019

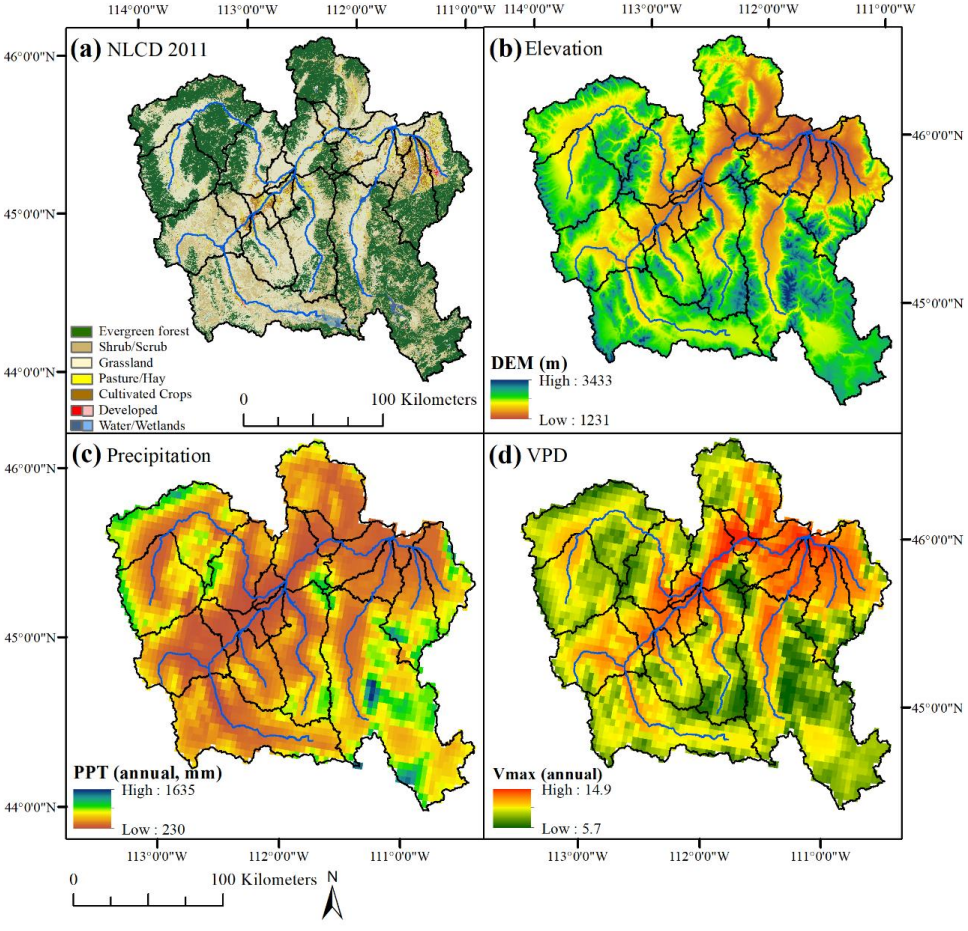

Figure 2. Spatial variability in (a) landcover, defined using the 2011 National Land Cover Database (NLCD), (b) elevation, (c) mean annual precipitation (PPT), and (d) mean annual vapor pressure deficit (VPD), across the Upper Missouri River Headwaters Basin. DEM: Digital Elevation Model, Vmax: maximum vapor pressure deficit.

2.2 Unit of Analysis

The objective of this study was not to document changes in the total amount of riparian vegetation, but instead to document temporal variability and trends in the wetness of persistent riparian vegetation in relation to climate and landscape variables. The extent of persistent riparian vegetation in major river valleys was delineated manually using Landsat imagery from 1985, 1986, 2016, and 2017 (Table 1) to define our area of analysis. National Agricultural Imaging Program (NAIP) imagery was also used to improve accuracy in areas where agriculture was inter-mixed with riparian vegetation. For headwater reaches, riparian areas upstream of all

Hydrol. Earth Syst. Sci. Discuss., https://doi.org/10.5194/hess-2019-137
Manuscript under review for journal Hydrol. Earth Syst. Sci.
Discussion started: 18 April 2019

identifiable irrigated agriculture were excluded from the analysis. For trend analysis, we used river topology, topography, and clusters of irrigated agriculture to divide the delineated riparian areas into 19 study reaches (Table 2, Fig. 2). After riparian reach lengths were defined, the per reach contributing area was calculated using the Spatial Tools for the Analysis of River Systems (STARS, v 2.0.4) (Peterson, 2017). All pits and flow interruptions in the digital elevation model (DEM) were filled. The flow direction for the river network was generated and the rivers burned into the DEM. The area contributing to the downstream point of each riparian reach (n=19) was estimated so that each contributing area was non-overlapping with edge-matching inter-basins (Theobald et al., 2006) (Table 2, Fig. 1).

Table 1. Landsat images used to map agricultural extent. The Palmer Hydrological Drought Index (PHDI) values were provided for the month of July. The percent was calculated based on the values that occurred between 1984 and 2017. TM: Thematic Mapper, OLI: Operational Land Imager

Date	Path/Row	Sensor	PHDI (%)
6-Aug-85	p39r28	TM	-2.85 (12.6)
6-Aug-85	p39r29	TM	-2.85 (12.6)
31-Jul-86	p40r28	TM	0.33 (43.0)
31-Jul-86	p40r29	TM	0.33 (43.0)
2-Aug-16	p40r28	OLI	-2.22 (19.3)
2-Aug-16	p40r29	OLI	-2.22 (19.3)
29-Jul-17	p39r28	OLI	-1.03 (35.2)
29-Jul-17	p39r29	OLI	-1.03 (35.2)

Hydrol. Earth Syst. Sci. Discuss., https://doi.org/10.5194/hess-2019-137
Manuscript under review for journal Hydrol. Earth Syst. Sci.
Discussion started: 18 April 2019

205 **Table 2.** Characteristics of each riparian reach considered including river length, riparian area analyzed, riparian reach contributing
206 area, and average (1984-2016) growing-season (June, July, August, JJA) Normalized Difference Wetness Index (NDWI) and
207 Normalized Difference Vegetation Index (NDVI). Standard error shown in parentheses.

Reach Code	River	River Length (km)	Riparian Area (ha)	Reach Contributing Area (km^2)	Total Upstream Contributing Area (km^2)	NDWI (JJA)	NDVI (JJA)
JR1	Jefferson River	55.4	1190	1021	24711	0.17 (0.01)	0.38 (0.01)
JR2	Jefferson River	25	745	395	21233	0.22 (0.01)	0.41 (0.01)
JR3	Jefferson River	48.9	1080	1348	20839	0.22 (0.01)	0.41 (0.01)
BVHR1	Beaverhead River	47.9	805	377	8867	0.20 (0.01)	0.47 (0.01)
BVHR2	Beaverhead River	34.3	352	345	8491	0.26 (0.01)	0.51 (0.01)
BVHR3	Beaverhead River	24	218	544	6774	0.21 (0.01)	0.48 (0.01)
BVHR4	Beaverhead River	93.8	160	2236	6230	0.26 (0.01)	0.50 (0.01)
RRR	Red Rock River	158	410	3993	3993	0.27 (0.01)	0.50 (0.01)
BTDR	Black Tail Deer River	77	26	1373	1373	0.22 (0.01)	0.45 (0.01)
RR	Ruby River	180.2	813	2726	2726	0.27 (0.01)	0.49 (0.01)
BHR1	Big Hole River	29.9	800	317	7898	0.20 (0.01)	0.43 (0.01)
BHR2	Big Hole River	64	850	1838	7581	0.23 (0.01)	0.42 (0.01)
BHR3	Big Hole River	104.6	1623	3259	5743	0.12 (0.01)	0.37 (0.01)
BHR4	Big Hole River	75.3	1717	2484	2484	0.17 (0.01)	0.49 (0.01)
MR1	Madison River	53.7	1072	886	8231	0.22 (0.01)	0.40 (0.01)
MR2	Madison River	108	1771	7345	7345	0.22 (0.01)	0.38 (0.01)
GR1	Gallatin River	20.9	495	310	3427	0.23 (0.01)	0.45 (0.01)
GR2	Gallatin River	54.4	1058	1660	1660	0.29 (0.01)	0.53 (0.01)
EGR	East Gallatin River	73	602	1457	1457	0.24 (0.01)	0.52 (0.01)

208

Hydrol. Earth Syst. Sci. Discuss., https://doi.org/10.5194/hess-2019-137
Manuscript under review for journal Hydrol. Earth Syst. Sci.
Discussion started: 18 April 2019

209 **2.3 Dependent Variable**

210 The NDWI calculated from Landsat imagery (NIR – SWIR1)/(NIR + SWIR1) (Gao,
211 1996; McFeeters, 1996) was used to estimate riparian wetness. Relative to other indices such as
212 the NDVI, NDWI is considered to be less sensitive to atmospheric conditions including solar
213 elevation angle, sensor angle, and atmospheric condition, making it suitable for time series
214 analysis (Crétaux et al., 2015), and has been used to monitor patterns in waterlogged areas
215 (e.g., Chatterjee et al., 2005; Chowdary et al., 2008). NDWI values greater than approximately
216 0.3 are typically used to distinguish open water (Chatterjee et al., 2005; Chowdary et al., 2008;
217 McFeeters, 2013). Across the UMH Basin, we determined that riparian NDWI values were more
218 sensitive to interannual variability in climate (Fig. 3) and river discharge than NDVI, making it a
219 more appropriate index for this analysis. Per year, average NDWI values (June – August, 1984-
220 2017, 102 values per riparian reach) were calculated using the Landsat surface reflectance image
221 collections in Google Earth Engine for all delineated riparian reaches (n=19). June, July and
222 August were selected to correspond to peak months for irrigation water withdrawals (Bauder,
223 2018). Potentially erroneous values were defined as values that were greater or less than plus or
224 minus two standard deviations from the riparian reach-specific mean monthly and were removed.
225 To normalize the data for seasonal variation values were calculated as the anomaly from the
226 riparian reach specific, long-term (1984-2017) mean monthly value (NDWI anomaly), then
227 averaged summer values (June-August) to provide a single NDWI anomaly per summer, per
228 reach. The multi-month approach compensated for data gaps created when cloud cover masked
229 Landsat NDWI values.
230
231 **2.4 Independent Variables**

232 Climate variables derived from the Parameter-elevation Regressions on Independent
233 Slopes Model (PRISM, Daly et al., 2008) included annual precipitation, annual lagged (one year)
234 precipitation, winter precipitation (January-March), spring precipitation (March-May), summer
235 precipitation (June-August), spring maximum and minimum temperature (March-May), summer
236 maximum and minimum temperature (June-August), maximum vapor pressure deficit (VPD;
237 spring and summer). VPD represents a measure of the drying power of the air and is a function
238 of air temperature and humidity. Across the contributing area of each riparian reach (n=19), 100
239 points were randomly selected (total points = 1900). To generate basin-wide values, the climate

values for each year (1984-2016) were extracted for each point, averaged for the reach (Table 3), then weighted using the relative size (ha) of each reach across the basin. Because upstream climate, such as snowfall or precipitation, can influence downstream riparian wetness, climate variables for each riparian reach were similarly calculated using the area-weighted average values for that reach and all reaches contributing to that reach.

To characterize interannual variability in snowfall, we used a total of 13 Snow Telemetry (SNOTEL) sites (IDs: 315, 318, 328, 355, 381, 403, 448, 568, 576, 578, 603, 656, 858). Annual total snowfall (September – August) and total spring snowfall (March-July) were calculated for each SNOTEL site (Table 3). For each riparian reach we identified the nearest one or two SNOTEL sites, using the SNOTEL site immediately upstream from the riparian reach as available. When two SNOTEL sites were used, the snowfall amounts were averaged across the two sites. Only sites with data available for the entire period of 1984-2017 were used (NSIDC, 2018). To further characterize climate conditions, we included the monthly Palmer Drought Severity Index (PDSI) and the Palmer Z-Index for NOAA NCDC Division 2 in Montana (Table 3). Both indices are calculated from precipitation and temperature station data and interpolated at 5 km (NOAA NCDC 2014). The PDSI represents the accumulation or deficit of water over the past approximately 9 months, while the Palmer Z-Index represents the current monthly conditions with no memory of previous deficits or surpluses (NOAA NCDC 2014). The indices were averaged to spring (March-May), summer (June-August), and annual, and represent multi-month averages of the drought indices. Temporal trends (1984-2016) in the climate variables were tested at the basin scale using the non-parametric Mann-Kendall test for trends (Kendall R package) (Mann, 1945, Kendall, 1975, Gilbert, 1987). Each SNOTEL site was tested independently for temporal trends in snowfall.

2.5 Agricultural Patterns

We sought to relate patterns in riparian wetness to patterns in total irrigated agricultural area and the relative abundance of irrigation methods. The USGS Water Use Surveys track surface and groundwater withdrawals and uses every five years (1950-2015) at a county scale (USGS 1988; Dieter et al., 2018). In both 1985 and 2015, 99% of water-withdrawals were surface water, and 99% of the total water withdrawals (surface + groundwater) were for irrigation across Beaverhead, Gallatin, Jefferson and Madison counties (USGS 1988; Dieter et

al., 2018). Across these counties total water withdrawals were 3% less in 2015 relative to 1985, although this pattern was variable across the basin with the Gallatin and Madison counties showing a 27% and 9% increase in water withdrawals, respectively, and the Jefferson and Beaverhead counties showing a 48% and 15% decrease in water withdrawals, respectively (USGS, 1988; Dieter et al., 2018). Across the UMH Basin, the Montana Department of Revenue's Final Land Unit Classification (FLU, 2010 and 2017) provides spatially explicit data on the irrigation methods used per field, while the U.S. Department of Agriculture's (USDA) CropScape (2007-2017) provides annual data on the spatial extent and crop type of agriculture. Between 2010 and 2017, the Montana State's FLU dataset documented a 1.6% increase in total irrigated agriculture, but a 17% increase in the area irrigated by center pivot irrigation.

These sources of data, however, lacked a spatially explicit dataset of agricultural extent and irrigation methods for the early part of the Landsat archive (1980s). Therefore, we generated two agricultural extent datasets representing the two temporal ends of the Landsat archive (1985/1986 and 2016/2017). The Landsat images used to define the active cropland extent are shown in Table 1. Cloud cover was only present in the mountainous areas in all images used. We recognize that by using a single Landsat image (instead of multiple images collected over the growing-season) and only representing the ends of the study time span, we may be underestimating agricultural extent and missing year-to-year variability in agricultural activities. Generating agriculture extent and irrigation types for the beginning and end of our study period, however, enabled us to identify spatially explicit trends or shifts in agricultural practices that have been previously shown at a county/state scale (USDA, 2018). Cropland extent was generated initially using eCognition 9.2 software (Trimble, Westminster, CO). The Landsat images were segmented into objects using the near infrared (NIR), red, and green bands. The FLU 2017 data layer was used to mask out non-crop and non-pasture land cover types. The objects were classified as agriculture or non-agriculture using NDVI thresholds. The draft agricultural outputs were then manually edited to add and remove agricultural fields as needed. Fallow fields were not included in the agricultural extent as they were assumed to be non-irrigated for that year. For overlapping portions between adjacent Landsat images, a field was included as crop if it was identified as such in either image.

Hydrol. Earth Syst. Sci. Discuss., https://doi.org/10.5194/hess-2019-137
Manuscript under review for journal Hydrol. Earth Syst. Sci.
Discussion started: 18 April 2019

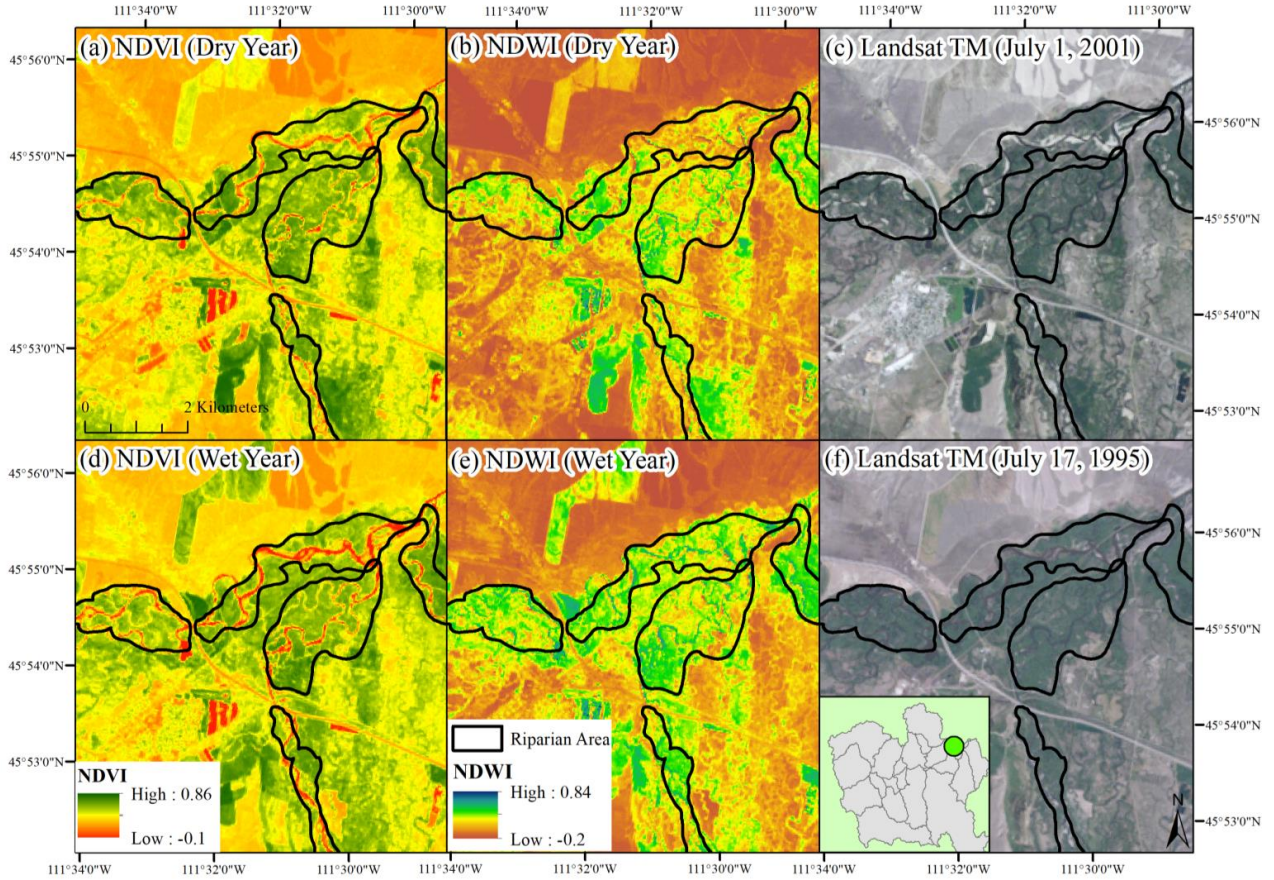

Figure 3. A visual comparison of index values in a dry year (2001, 431 mm annual precipitation) and a wet year (1995, 687 mm annual precipitation) at the confluence of Jefferson, Madison and Gallatin Rivers. The Normalized Difference Wetness Index (NDWI) in the riparian vegetation showed more variability in response to precipitation relative to the Normalized Difference Vegetation Index (NDVI). A comparison of (a) NDVI (July 2001), (b) NDWI (July 2001), (c) raw Landsat image (July 1, 2001), (d) NDVI (July 1995), (e) NDWI (July 1995), and (f) raw Landsat image (July 17, 1995). A similar pattern was observed across the basin.

306 **Table 3.** Climate variables considered in the analysis to represent interannual variability in conditions. The 25th, 50th, and 75th quartile
307 are shown to indicate the variability in the per-riparian reach values included in the random forest (RF) regressions (n=19). The
308 frequency of variable selection for inclusion in the random forest regressions is also shown. When tested at a basin-scale for the time
309 period of 1984-2016, no climate variables showed a significant temporal trend except summer vapor pressure deficit (* = p<0.1).
310 PRISM: Parameter-elevation Regressions on Independent Slopes Model, SNOTEL: snow telemetry, NOAA: National Oceanic and
311 Atmospheric Administration, summer: (June, July, August), spring: (March, April, May)

Climate Variables	Source	25th quartile	50th quartile	75th quartile	Temporal Trend (tau)	Frequency selected for inclusion in RF regressions
Annual precipitation (mm)	PRISM	456.1	527.1	620.4	-0.03	11
1-year lagged annual precipitation (mm)	PRISM	458.9	532.7	625.4	-0.03	2
Precipitation (spring) (mm)	PRISM	48.1	56.2	68.0	-0.004	1
Precipitation (summer) (mm)	PRISM	32.7	43.8	58.1	-0.13	4
Annual snowfall (snow water equivalent (SWE), mm)	SNOTEL	938.6	1113.4	1421.0	-0.18 - 0.16	1
Spring snowfall (March-June) (SWE, mm)	SNOTEL	169.3	264.7	402.3	-0.18 - 0.15	7
Maximum temperature (spring) (°C)	PRISM	9.7	11.1	12.4	-0.03	3
Maximum temperature (summer) (°C)	PRISM	23.4	24.6	25.8	-0.03	1
Minimum temperature (spring) (°C)	PRISM	-4.2	-3.1	-2.0	-0.004	0
Minimum temperature (summer) (°C)	PRISM	5.3	6.4	7.5	-0.13	0
Vapor Pressure Deficit maximum (spring)	PRISM	7.1	8.1	9.0	0.07	8
Vapor Pressure Deficit maximum (summer)	PRISM	18.4	20.5	22.7	0.21*	6
Palmer Z-Index (annual)	NOAA	-0.5	-0.3	0.3	-0.07	9
Palmer Drought Severity Index (annual)	NOAA	-1.6	-0.2	0.8	-0.11	13
Palmer Z-Index (spring)	NOAA	-0.9	0.2	0.8	0.02	9
Palmer Drought Severity Index (spring)	NOAA	-1.8	-0.3	1.1	-0.05	8
Palmer Z-Index (summer)	NOAA	-1.5	-0.4	1.0	-0.15	5
Palmer Drought Severity Index (summer)	NOAA	-2.4	-0.5	1.3	-0.14	15

312
313
314

Hydrol. Earth Syst. Sci. Discuss., https://doi.org/10.5194/hess-2019-137
Manuscript under review for journal Hydrol. Earth Syst. Sci.
Discussion started: 18 April 2019

Active crop fields were further classified manually as center pivot irrigation or non-center pivot irrigation (e.g., gravity-fed, non-center pivot sprinkler) based on field shape (i.e., round, not round). There may be potential confusion between non-center pivot irrigation and non-irrigated fields, however, 92 and 93% of the 1985/1986 and 2016/2017 agricultural area, respectively, co-occurred with FLU polygons classified as irrigated, suggesting that non-irrigated agriculture is a minority cover class across the UMH basin. For reference, the FLU polygons were classified as center-pivot, sprinkler or gravity-fed using irrigation infrastructure (gates, ditches, dikes) identifiable from National Agricultural Imaging Program (NAIP) images (1 m resolution). Sprinkler irrigation was distinguished using parallel wheel lines. Our efforts, in contrast, did not attempt to distinguish gravity-fed irrigation from non-center pivot sprinkler irrigation.

2.6 Analysis

Temporal trends in riparian wetness (NDWI anomaly ~ Year) were tested for each riparian reach using the non-parametric Mann-Kendall (MK) test for trends. As the MK test for trends can be sensitive to temporal autocorrelation (Hamed and Rao, 1998), we used the Durbin-Watson statistic to test for the presence of temporal autocorrelation in the NDWI anomaly values of each riparian reach (Table 4). Temporal autocorrelation was found to be significant for the NDWI anomaly data over time in 3 of the 19 riparian reaches, but in all three cases, the autoregressive model (AR1) performed worse than the linear model, as evaluated by comparing Akaike Information Criterion (AICc) values (Hurvich and Tsai, 1989), suggesting that autoregressive models were not appropriate for this analysis (Table 4). However, because autocorrelation can inflate trend significance, for these three riparian reaches we calculated a modified Mann-Kendall test for trends that accounts for the autocorrelation structure of the data (Hamed and Rao, 1998).

Interannual variability in riparian wetness for a given reach can be expected to be a function of (1) interannual climate variability and (2) changes in the amount and timing of anthropogenic water withdrawals or water return flow, while spatial variability in these relationships can be expected to be a function of landscape characteristics. Temporal variability in climate and anthropogenic activities could occur both within each reach and upstream of each reach. Because annual (1984-2016) agricultural and irrigation data were not available for the

entire time series, the influence of water withdrawals was estimated as the residual variance after modeling the interannual variability in riparian wetness attributable to climate.

The NDWI anomaly values were related to climate variables for each riparian reach using random forest analysis. The random forest analyses were used to quantify the amount of variation in the NDWI anomalies explained by climate variables and to identify the frequency (importance) of particular climate variables in predicting NDWI anomalies. Random forest techniques use bootstrapping to employ hundreds of regression trees and make no prior assumptions about cause and effect relationships or correlations among variables (Hastie et al., 2009). Random forest techniques are generally insensitive to multicollinearity; however, the inclusion of highly correlated variables can deflate both variable importance and the overall variation explained by the analysis, while the inclusion of many variables can make interpretation difficult and introduce noise (Murphy et al., 2010). We therefore implemented variable selection using the *rfUtilities* package in R (Murphy et al., 2010) before running random forest regressions for each riparian reach with the selected subset of climate variables. To model growing-season riparian NDWI anomalies we calculated 500 regression trees for each riparian reach. Although we did not restrict the number of nodes, model overfit was limited by setting the minimum sample size per node to 5. Because of the limited data points per riparian reach (n=33) model fit was assessed using out of bag (OOB) root mean squared error (RMSE, 70% of points used to train, 30% of points used to validate) using the *randomForest* package in the R statistical software (Liaw and Wiener, 2015). We found no increase in the OOB error as more trees were generated (i.e., up to 500 trees). Random forest regression residuals were then extracted and evaluated for temporal trends not attributable to climate variability (NDWI anomaly random forest regression residuals ~ Year). Temporal trends in the regression residuals were tested using the non-parametric MK test for trends. We again used the Durbin-Watson statistic to test for the presence of temporal autocorrelation in the NDWI anomaly-climate regression residual values of each riparian reach (Table 4). Temporal autocorrelation was found to be significant for the residual data over time in 3 of the 19 riparian reaches, so the modified Mann-Kendall test for trends, that accounts for the autocorrelation structure of the data (Hamed and Rao, 1998), was used for these three riparian reaches. Differences in agriculture between riparian reaches that showed a trend in the NDWI anomaly-climate regression residuals and riparian reaches that did not were compared using the non-parametric Mann-Whitney-Wilcoxon Test.

We note that we tested an alternative method in which data for all riparian reaches and years were combined in a single linear mixed model. Although this approach increased our sample size (33 years x 19 riparian reaches), we found that the error in the regression, specifically the strength of the relationship between the predicted and actual NDWI anomalies, was uneven between riparian reaches, thereby decreasing our confidence in the analysis of trends in the residuals. This finding further supported our decision to run a random forest regression for each riparian reach.

2.7 Ancillary Spatial Datasets

Landscape characteristics such as topography, geology, and landcover may influence how riparian vegetation responds to climate variability over time and were therefore also considered. Between-group differences in landscape characteristics were calculated for riparian reaches that showed a temporal trend in riparian wetness relative to riparian reaches that showed no temporal trend in riparian wetness using the non-parametric Mann-Whitney-Wilcoxon Test (or the Wilcoxon rank sum test) (Cohen, 1988). Variability in topography was quantified as the (1) elevation coefficient of variation across each 10-digit hydrologic unit code (HUC-10) (Ascione et al., 2008), as well as the (2) Melton Ruggedness number, which is calculated as the maximum elevation minus the minimum elevation divided by the area of the hydrological unit (HUC10) (Melton, 1965), using the USGS National Elevation Dataset (NED) 10 m resolution (Gesch et al., 2002). The percent of the riparian reach's within reach contributing area that was (1) evergreen forest, (2) herbaceous vegetation, (3) pasture, and (4) crop was included, as classified by the National Land Cover Database (NLCD) 2011 (Homer et al., 2015). Soil and geology characteristics were considered using the minimum water table depth (April-July), bedrock depth, and soil drainage characteristics, specifically the percent of each riparian reach's contributing area that is well drained (excessively drained, somewhat excessively drained, well drained) and poorly drained (very poorly drained, poorly drained). These variables were derived from the National Resources Conservation Service's Soil Survey Geographic (SSURGO) database to characterize infiltration capacity (Soil Survey Staff, 2018). Change in developed (built-up) land, including urban, residential, and commercial land uses was quantified using the "Historical built-up intensity layer (1810-2015, 5-year intervals)" (Leyk and Johannes, 2018). This dataset quantifies the sum of building areas of all structures per pixel, where pixel size is

250 m by 250 m. Change in built-up intensity was quantified as the change in the sum of building areas between 2015 and 1985 (m^2) per river length (m).

2.8 River Discharge

Riparian corridors are interconnected with its adjacent rivers via longitudinal, lateral, and vertical fluxes of water (Fritz et al., 2018). To explore the potential relationship between riparian water storage and river discharge across the UMH Basin, we identified seven USGS stream gages within the basin with upstream contributing areas ranging between ~3,400 ha and ~25,000 ha (Table 5). The gages were variable in their position relative to flow regulators such as dams associated with lakes or reservoirs (Table 5). The amount of flow regulation enforced by these flow regulators was unknown and therefore a point of uncertainty. The Spearman correlation coefficient was calculated between the monthly river discharge, averaged to June-August, and the riparian NDWI for the co-located riparian reach or the riparian reach immediately adjacent to each gage. We note that a correlation can be indicative of a similar response of both variables to interannual water availability (e.g., precipitation) as well as potential movement of water across the river-upland interface. We also evaluated trends in river discharge over time (1984-2016) in growing-season (June, July, August), as well as autumn (September, October, and November) and winter (December, January, February) seasons using the MK test for trends. The temporal trends in river discharge were calculated only to compare with temporal trends in riparian wetness over the same period. We note that a full trend analysis in river discharge would require not only utilizing the entire record of river discharge available per gage, but also considering the potential impact of flow regulation via dams, as well as interannual variability in surface withdrawals for irrigation, which are closely regulated by Montana State Law (Montana DNRC, 2015).

Hydrol. Earth Syst. Sci. Discuss., https://doi.org/10.5194/hess-2019-137
Manuscript under review for journal Hydrol. Earth Syst. Sci.
Discussion started: 18 April 2019

Hydrology and Earth System Sciences
Discussions

433 **Table 4.** Temporal trends in per reach riparian Normalized Difference Wetness Index (NDWI,
434 June, July, August) anomalies using the Mann-Kendall (MK) test for trends. The Durbin-Watson
435 (DW) statistic was used to test for the presence of temporal autocorrelation. NDWI anomalies
436 were modeled against climate variables using random forest regressions. The temporal trends in
437 the random forest regression residuals were evaluated using MK test for trends. A modification
438 of the MK (Hamed and Rao, 1998) was used for the reaches where the DW statistic was
439 significant. RMSE: root mean square error, **: p<0.05, *: p<0.1

Reach Code	River	NDWI anomaly DW statistic	NDWI anomaly MK tau	Random forest R^2 value	Random Forest RMSE	Residual DW statistics	Residual MK tau
JR1	Jefferson River	1.56	-0.22*	0.65**	0.02	1.74	-0.28**
JR2	Jefferson River	2.13	-0.10	0.48**	0.03	2.58	-0.15
JR3	Jefferson River	1.75	-0.20	0.66**	0.02	2.13	-0.27**
BVHR1	Beaverhead River	1.51	-0.35**	0.53**	0.03	1.36**	-0.27**
BVHR2	Beaverhead River	1.77	-0.08	0.56**	0.03	1.84	-0.03
BVHR3	Beaverhead River	1.28**	-0.39**	0.25**	0.04	1.83	-0.26**
BVHR4	Beaverhead River	1.40**	-0.36**	0.47**	0.04	1.51	-0.36**
RRR	Red Rock River	1.63	-0.20	0.32**	0.03	1.61	-0.16
BTDR	Black Tail Deer River	1.57	-0.35**	0.48**	0.04	1.87	-0.30**
RR	Ruby River	1.84	-0.21*	0.34**	0.03	2.05	-0.21*
BHR1	Big Hole River	1.64	-0.16	0.64**	0.02	1.68	-0.15
BHR2	Big Hole River	2.33	0.06	0.47**	0.02	2.05	0.16
BHR3	Big Hole River	2.01	-0.06	0.69**	0.02	2.37	-0.03
BHR4	Big Hole River	2.13	-0.02	0.28**	0.05	2.88**	-0.08
MR1	Madison River	2.18	-0.23*	0.54**	0.02	2.32	-0.26**
MR2	Madison River	2.47	-0.10	0.58**	0.02	2.40	-0.05
GR1	Gallatin River	2.02	-0.38**	0.37**	0.03	2.23	-0.53**
GR2	Gallatin River	1.97	-0.16	0.23**	0.02	1.68	-0.09
EGR	East Gallatin River	2.68*	-0.11	0.46**	0.02	2.69*	-0.16

440

Hydrol. Earth Syst. Sci. Discuss., https://doi.org/10.5194/hess-2019-137
Manuscript under review for journal Hydrol. Earth Syst. Sci.
Discussion started: 18 April 2019

Table 5. River discharge characteristics for the U.S. Geological Survey (USGS) gages used in the analysis. Summer (June, July, August) discharge was correlated with the summer Normalized Difference Wetness Index (NDWI) and spring snowfall (March-June) for the riparian reach adjacent to each gage, using the Spearman correlation. Temporal trends were quantified using the Mann-Kendall test for trends. Percent discharge consumed and diverted is from the 2014 Water Plan (MT DNRC, 2014). JJA: June, July, August, SON: September, October, November, DJF: December, January, February, D: dam present at gage, D-US: dam upstream, ND: no dam or minimal flow regulation, na: data not available, SE: standard error, **: $p<0.05$, *: $p<0.1$

					Seasonal mean river discharge (m^3 sec^{-1}; ±SE)		
Station ID	**USGS Gage Name**	**Reach Code**	**Contributing Area (ha)**	**Consumed (%) / Diverted but not consumed (%)**	**Summer (JJA)**	**Autumn (SON)**	**Winter (DJF)**
6036650	Jefferson River near Three Forks, MT	JR1	24692	6% / 20%	68.3 (8.3)	35.0 (2.5)	33.0 (1.5)
6018500	Beaverhead River near Twin Bridges, MT	BVHR1	8490	29% / 69%	5.7 (1.7)	9.0 (1.2)	8.8 (0.7)
6025500	Big Hole River near Melrose, MT	BHR2	7581	13% / 43%	44.3 (4.5)	11.4 (0.5)	10.1 (0.4)
6041000	Madison River below Ennis Lake near McAllister, MT	MR2	7132	3% / 11%	56.9 (3.4)	44.5 (1.5)	38.5 (0.7)
6016000	Beaverhead River at Barretts, MT	BVHR3	6230		20.3 (1.5)	8.3 (1.2)	na
6052500	Gallatin River at Logan, MT	GR1	3426	13% / 37%	40.7 (3.6)	18.9 (0.7)	18.6 (0.4)
6024450	Big Hole River below Big Lake Creek at Wisdom, MT	BHR4	2058		7.9 (1.3)	1.6 (0.1)	na
		Correlation coefficient (r)			**Seasonal temporal trends (tau)**		
Station ID	**USGS Gage Name**	**NDWI (JJA)**	**Snowfall (March-June)**	**Flow Regulation**	**Summer (JJA)**	**Autumn (SON)**	**Winter (DJF)**
6036650	Jefferson River near Three Forks, MT	0.82**	0.89**	D-US	0.02	-0.16	-0.07
6018500	Beaverhead River near Twin Bridges, MT	0.57**	0.19	D-US	-0.01	-0.10	0.07*
6025500	Big Hole River near Melrose, MT	0.60**	0.84**	ND	0.12	0.07	0.16
6041000	Madison River below Ennis Lake near McAllister, MT	0.64**	0.79**	D	0.06	-0.33**	-0.33**
6016000	Beaverhead River at Barretts, MT	0.55**	0.51**	D	0.11	0.04	na
6052500	Gallatin River at Logan, MT	0.60**	0.69**	ND	0.00	-0.20*	-0.15
6024450	Big Hole River below Big Lake Creek at Wisdom, MT	0.55**	0.70**	ND	0.02	0.28**	na

Hydrol. Earth Syst. Sci. Discuss., https://doi.org/10.5194/hess-2019-137
Manuscript under review for journal Hydrol. Earth Syst. Sci.
Discussion started: 18 April 2019

3. Results

3.1 Trends in Riparian Wetness

A total of 15,785 ha (157.85 km^2) of riparian vegetation was delineated along the major rivers (Fig. 1). River length within each riparian reach ranged from 21 km along the Gallatin River to 180 km along the Ruby River, and averaged 70 km in length (Table 2, Fig. 1). The total riparian area analyzed per reach ranged from 26 ha (289 Landsat pixels) along the Black Tail Deer River to 1771 ha (19,678 Landsat pixels) along the Madison River, and averaged 831 ha (9,233 Landsat pixels, Table 2). The NDVI and NDWI averaged 0.45 and 0.22, respectively, across riparian reaches and years (Table 2). All 19 riparian reaches showed an average NDWI of <0.3 (Table 2), the threshold that is typically used to identify open water (Chatterjee et al., 2005; Chowdary et al., 2008; McFeeters, 2013).

When we tested for MK trends in growing-season (June-August) riparian wetness over time, 8 of the 19 riparian reaches showed a significant decline over time in growing-season NDWI anomalies (5 riparian reaches p<0.05, 3 riparian reaches p<0.1) (Table 4, Fig. 4). The BVHR3 and BVHR4 riparian reaches that tested positive for autocorrelation still showed a significant drying trend after using the modified MK test. Interannual variability in climate can be expected to explain a portion of the interannual variability in riparian wetness. Across all 19 reaches, climate variables explained 23 to 69% (averaged 47%) of the interannual variability in riparian NDWI anomalies (Table 4). However, basin-wide, the climate variables did not show a temporal trend over same period (1984-2016), apart from the VPD maximum (summer) which showed an increasing trend (p<0.1) (Table 3). Drought indices, in particular the PDSI (summer, selected in 15 regressions and annual, selected in 13 regressions), but also the Palmer Z-index (annual and spring both selected in 9 regressions), as well as annual precipitation (selected in 11 regressions) were the variables most frequently selected for inclusion in the random forest analyses (Table 3).

For the eight riparian reaches that showed a temporal trend in NDWI anomalies (Figure 4a) the NDWI anomaly-climate regression residuals also showed a significant negative trend over time, indicating that declines in riparian wetness cannot be attributed solely to climate variability (7 riparian reaches p<0.05, 1 riparian reach p<0.1, Table 4, Fig. 4b). One additional riparian reach along the Jefferson River (JR3) did not show a significant trend in NDWI anomalies but did show a significant negative trend in the NDWI anomaly-climate regression

Hydrol. Earth Syst. Sci. Discuss., https://doi.org/10.5194/hess-2019-137
Manuscript under review for journal Hydrol. Earth Syst. Sci.
Discussion started: 18 April 2019

Hydrology and Earth System Sciences
Open Access
Discussions

481 residuals (p<0.05, Table 4, Fig. 4). The riparian reach BVHR1 also showed a significant negative
482 trend in the NDWI anomaly-climate regression residuals when tested using the modified MK
483 test. Data for two of the riparian reaches at the basin outlet (JR1, GR1) are shown in Fig. 5 and
484 Fig. 6, respectively. Both show a decline in NDWI anomalies over time, with the slope of the
485 relationship steepening after the removal of the climate component (Fig. 5 and 6).

Hydrol. Earth Syst. Sci. Discuss., https://doi.org/10.5194/hess-2019-137
Manuscript under review for journal Hydrol. Earth Syst. Sci.
Discussion started: 18 April 2019

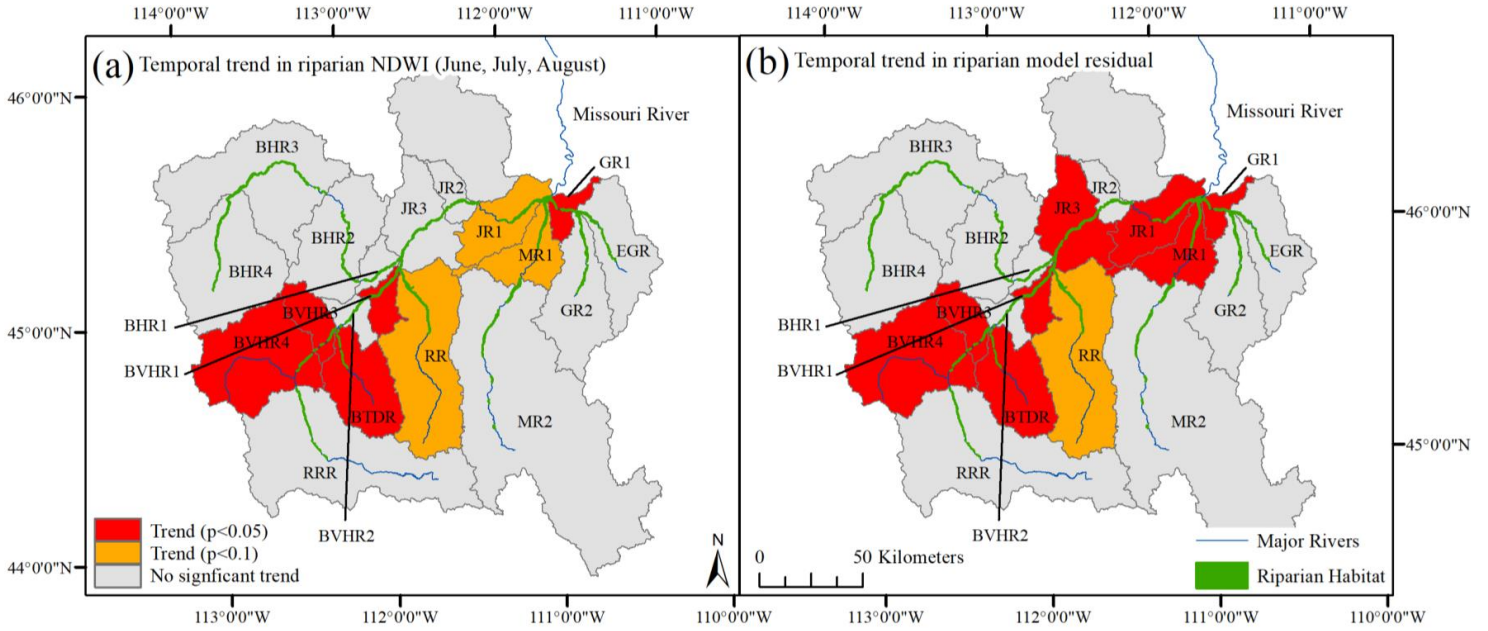

Figure 4. (a) The spatial distribution of riparian reaches found to show a significant decreasing trend (p<0.1 or p<0.05) in riparian wetness using the Normalized Difference Wetness Index (NDWI, June, July, August) anomalies, and (b) the spatial distribution of riparian reaches found to show a significant trend in NDWI anomaly-climate regression residuals, or the variance in NDWI anomalies not explained by climate variables. All trends were negative, indicating a drying over time.

Hydrol. Earth Syst. Sci. Discuss., https://doi.org/10.5194/hess-2019-137
Manuscript under review for journal Hydrol. Earth Syst. Sci.
Discussion started: 18 April 2019

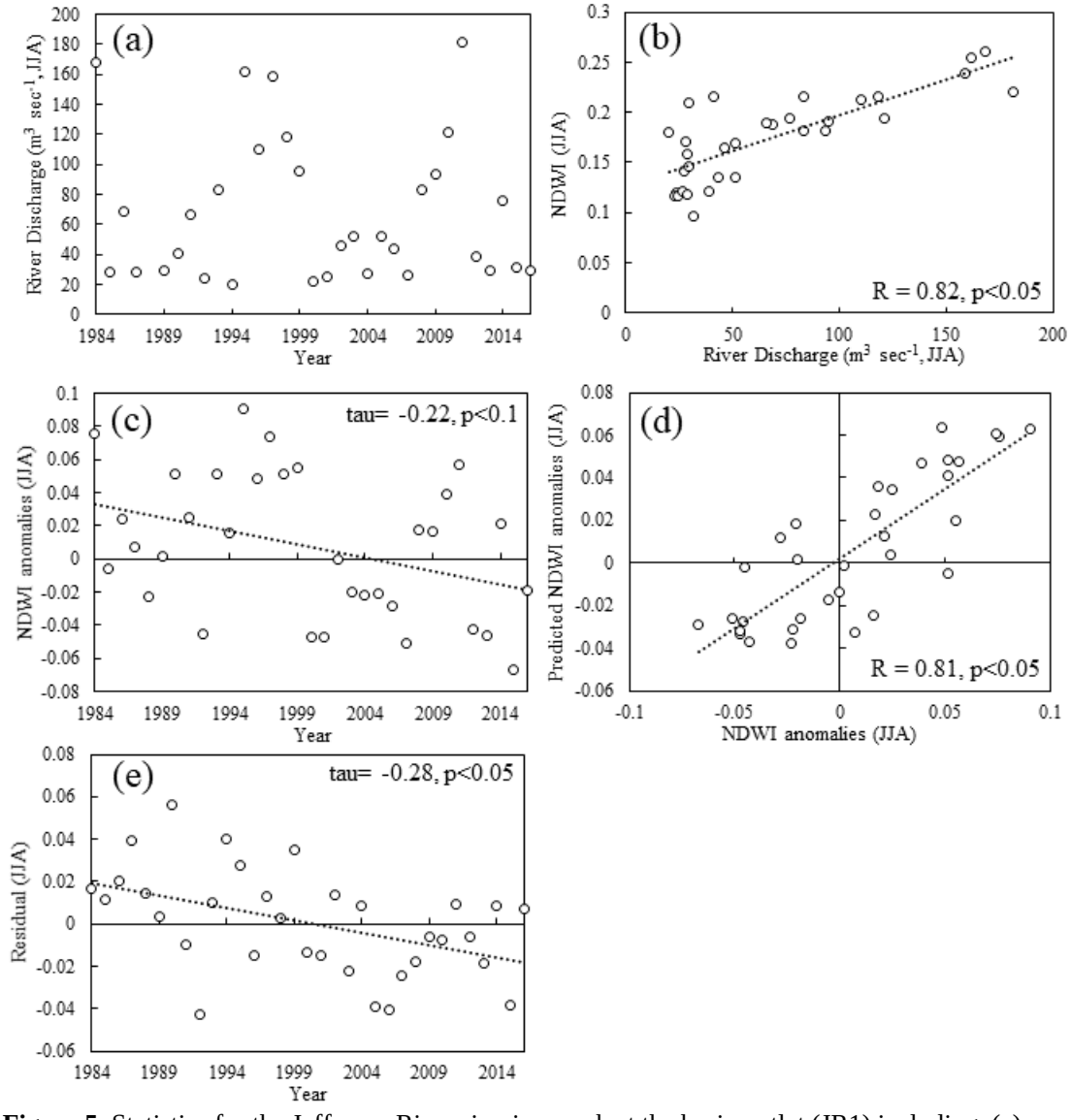

Figure 5. Statistics for the Jefferson River riparian reach at the basin outlet (JR1) including, (a) variability in June, July, August (JJA) river discharge over time (Station ID: 6036650), (b) relationship between the Normalized Difference Wetness Index (NDWI) and river discharge, (c) trend in NDWI anomalies over time, (d) correlation between NDWI anomalies and predicted NDWI anomalies, and (e) trend in NDWI anomalies-climate regression residuals over time.

Hydrol. Earth Syst. Sci. Discuss., https://doi.org/10.5194/hess-2019-137
Manuscript under review for journal Hydrol. Earth Syst. Sci.
Discussion started: 18 April 2019

499

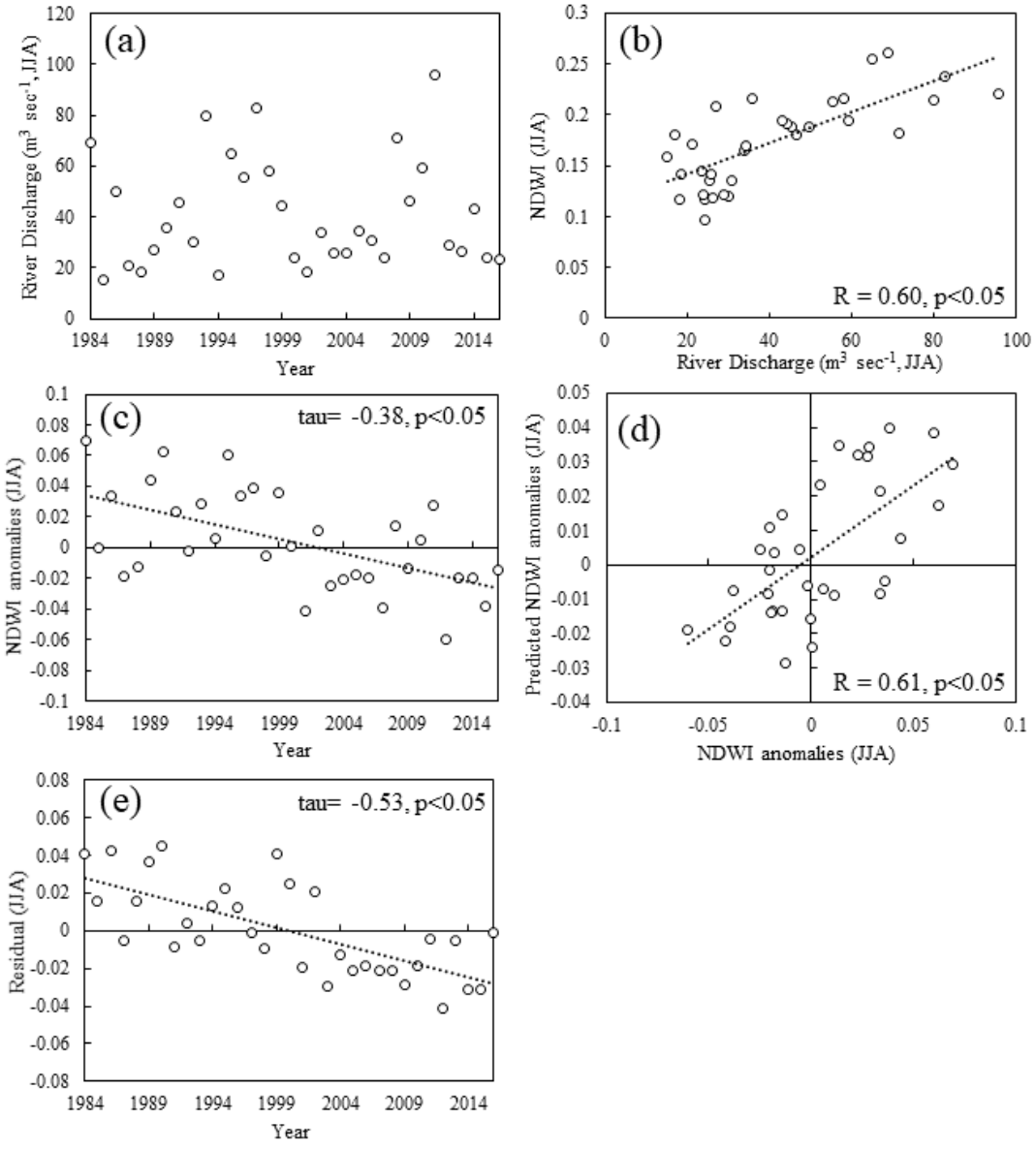

500
501 **Figure 6.** Statistics for the Gallatin River riparian reach downstream of the East Gallatin River
502 (GR1) including, (a) variability in river discharge over time (Station ID: 6052500), (b)
503 relationship between the Normalized Difference Wetness Index (NDWI) and river discharge, (c)
504 trend in NDWI anomalies over time, (d) correlation between NDWI anomalies and predicted
505 NDWI anomalies, and (e) trend in NDWI anomalies-climate regression residuals over time.
506
507

Hydrol. Earth Syst. Sci. Discuss., https://doi.org/10.5194/hess-2019-137
Manuscript under review for journal Hydrol. Earth Syst. Sci.
Discussion started: 18 April 2019

Hydrology and Earth System Sciences
Discussions

3.2 Trends in Agriculture and Water Withdrawals

Agriculture across the UMH Basin is spatially distributed along the major rivers (Fig. 2a). Using the endpoint (1985/86 and 2016/17) agriculture dataset, the largest amounts of agriculture occurred along the Gallatin River, Beaverhead River, Ruby River, and the most upstream reach of the Big Hole River (Fig. 7a). The effect of water withdrawals can be expected to accumulate downstream, therefore the total amount of upstream agriculture was highest along the Beaverhead River, Jefferson River and downstream portion of the Gallatin River (Fig. 7b). Over the study period the total amount of agriculture was relatively stable (4% increase), although we observed a minor decline in total agriculture across the most upstream portion of the basin, and the largest increases in total agriculture along the Gallatin and Jefferson Rivers (Fig. 7 and 8). In contrast, irrigation methods saw much greater changes. We observed a five-fold (506%) increase in the amount of agriculture using center pivot irrigation, and a 39% decrease in the amount of agriculture using non-center pivot irrigation (Table 6). Aerial imagery shows examples of the conversion to center pivot irrigation between 1985 and 2017 (Fig. 8). The percent change in agricultural land area using center pivot irrigation ranged from 0% to 58% across the reaches, with the biggest conversions along the Jefferson, Beaverhead, Madison and Black Tail Deer Rivers (Table 6). After controlling for river length, the Gallatin, Jefferson and Beaverhead saw the largest increases in center pivot agriculture. And the rate of conversion could help explain the drying trends. Riparian reaches that saw a significant decline in riparian wetness, even after accounting for variability explained by climate, showed a 46% average increase in the fraction of reach-scale center pivot irrigation relative to the 32% average increase in riparian reaches where no such temporal trend was observed (Mann-Whitney-Wilcoxon, $p<0.1$). Drying riparian reaches also had more agriculture within and upstream of them than non-drying reaches (269 km^2 relative to 171 km^2 of active agriculture), but this second difference was not statistically significant (Table 6).

The response of a riparian reach to changes in water withdrawals and irrigation method may also depend on other landscape characteristics such as soil, geology and topography. Riparian reaches that showed a significant non-climate related drying over time showed a higher percent well-drained soils ($p<0.05$) and higher Melton Ruggedness number (greater range in elevation per area, $p<0.05$, Table 7). In addition, although irrigation dominates water consumption across the basin, we note that development has increased around Bozeman, along

539 the East Gallatin River, over the study period, while minimal increases in development were
540 found elsewhere (Fig. 7F).
541 Although the examples in Fig. 5 and Fig. 6 fit the pattern of a shift towards center pivot
542 irrigation and a corresponding drying trend in riparian wetness, other reaches showed less
543 intuitive patterns. For instance, all reaches that showed a significant drying trend also showed a
544 substantial increase in the fraction of center pivot agriculture, ranging from 35% to 64%, except
545 BVHR4, which showed a significant drying trend without an associated increase in center pivot
546 agriculture (a 24% increase in center pivot agriculture, but the lowest total ha of center pivot
547 irrigation in 2016/17 of any riparian reach). The NDWI anomalies and NDWI anomalies-climate
548 residuals shown in Fig. 9a and 9b indicate that this stretch of the Beaverhead River (BVHR4),
549 which is immediately downstream from the Clark Canyon Reservoir, experienced a step decrease
550 in riparian wetness in 2002, with no visible trend before or after 2002. Such a clear step decrease,
551 however, was not observed in the closest stream gage (Station ID: 06016000) downstream of this
552 riparian reach. In contrast, one riparian reach on the Beaverhead River further downstream
553 (BVHR2) showed a 54% increase in the fraction of center pivot agriculture, as well as a decrease
554 in total agriculture over the study period (-48.5 ha km^{-1} river length), with no drying trend (Fig.
555 9c and 9d), even though reaches upstream and downstream of BVHR2 show significant drying
556 trends. With the landscape characteristics considered we were again unable to determine why
557 this riparian reach was more resilient than other riparian reaches of this river.
558

Hydrol. Earth Syst. Sci. Discuss., https://doi.org/10.5194/hess-2019-137
Manuscript under review for journal Hydrol. Earth Syst. Sci.
Discussion started: 18 April 2019

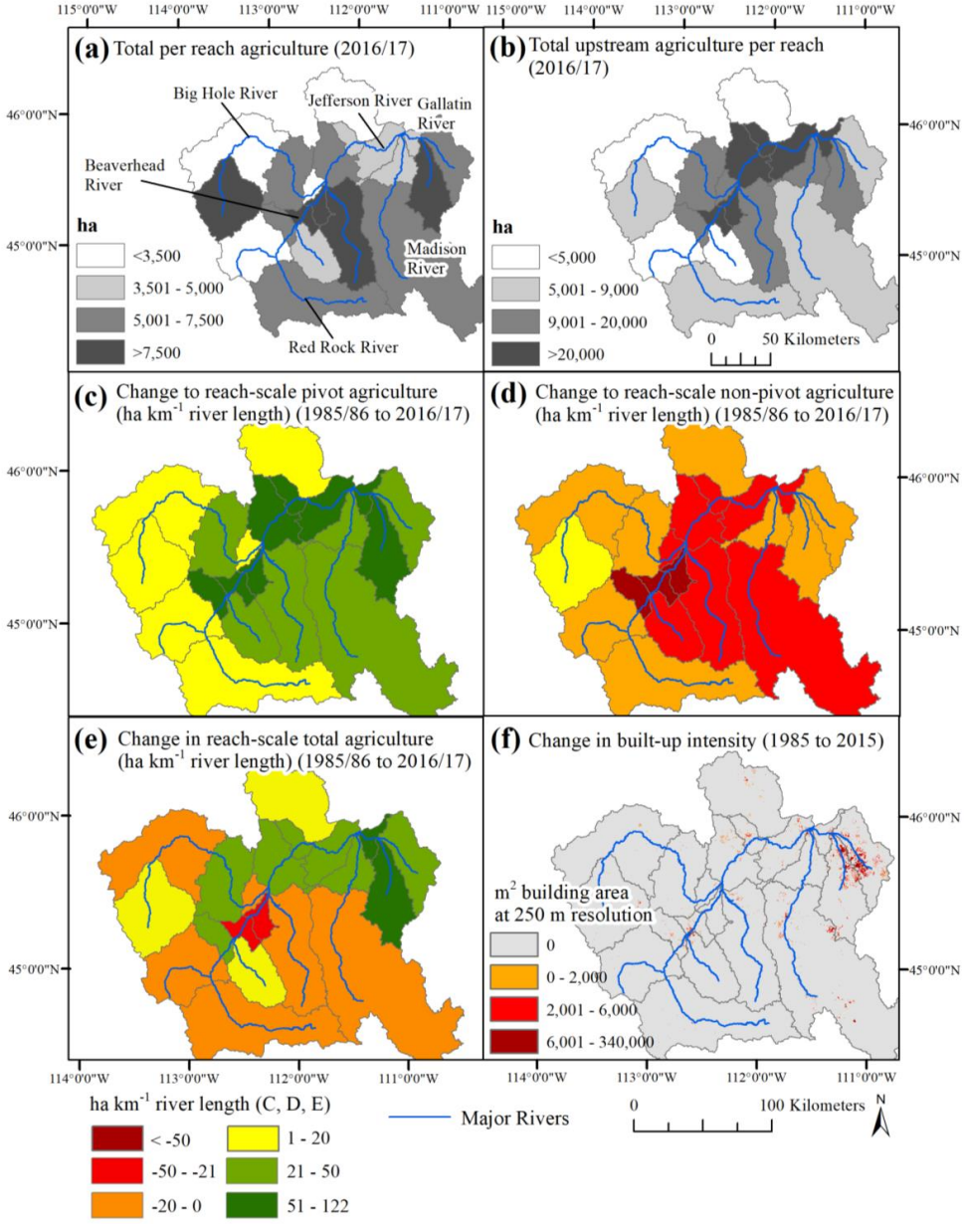

Figure 7. Changes in agricultural and development characteristics across Upper Missouri River Headwaters Basin between 1985/86 and 2016/17 including, (a) total per reach agriculture (2016/17), (b) total agriculture within and upstream of each reach (i.e., accumulated ag) (2016/2017), (c) change to reach-scale abundance of center pivot irrigated agriculture (1985/86 to 2016/17), (d) change to reach-scale abundance of non-pivot irrigated agriculture (1985/86 to 2016/17), (e) change in total per reach agriculture (1985/86 to 2016/17), and (f) change in built-up intensity, defined as the summed building area at 250 m resolution (1985 to 2015).

Hydrol. Earth Syst. Sci. Discuss., https://doi.org/10.5194/hess-2019-137
Manuscript under review for journal Hydrol. Earth Syst. Sci.
Discussion started: 18 April 2019

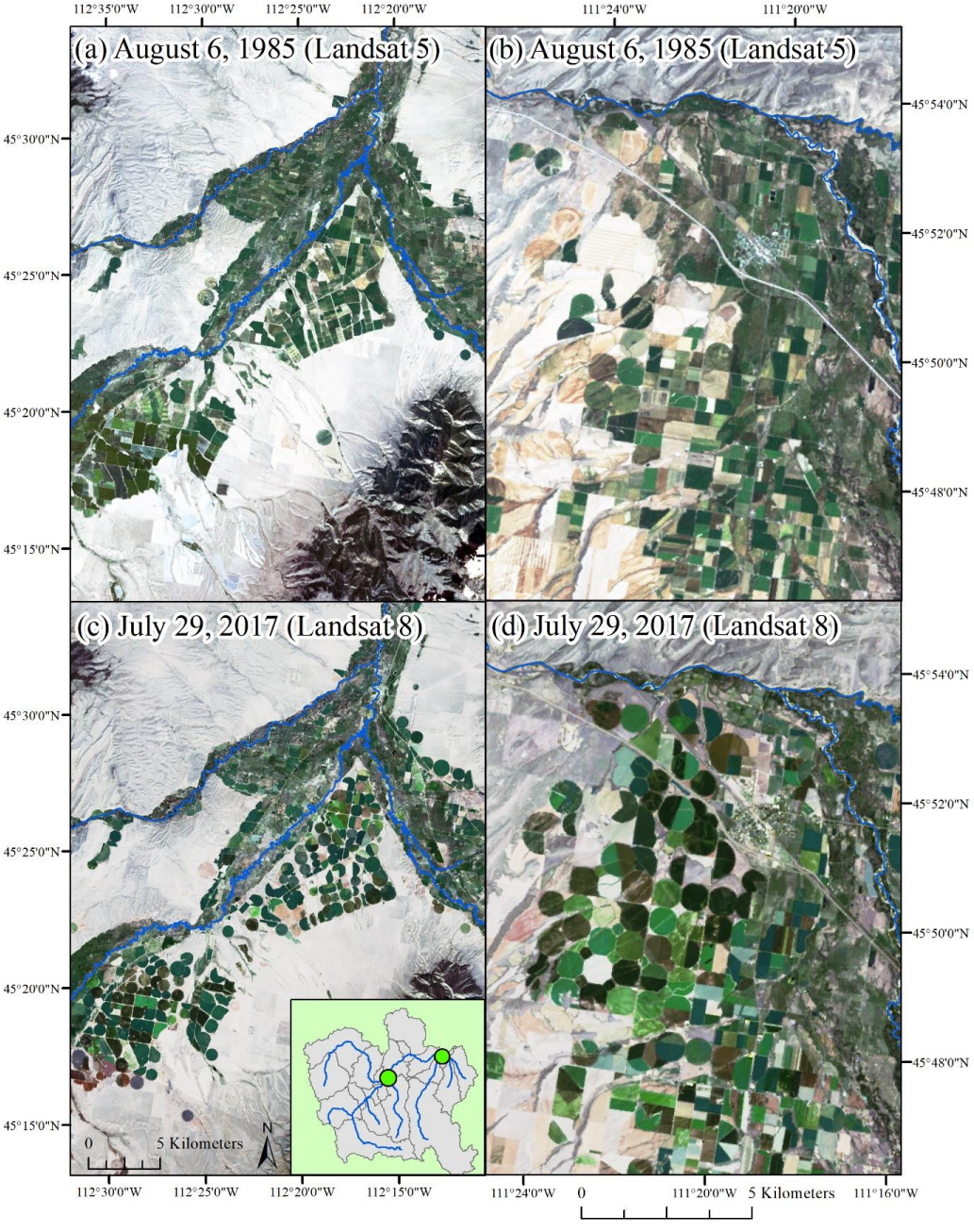

Figure 8. Examples of areas showing a shift in irrigation technique over the past 30 years across the Upper Missouri River Headwaters Basin including examples at the confluence of the Beaverhead (center), Big Hole (left), and Ruby River (right), shown in (a) and (c), as well as examples along Gallatin River shown in (b) and (d).

Hydrol. Earth Syst. Sci. Discuss., https://doi.org/10.5194/hess-2019-137
Manuscript under review for journal Hydrol. Earth Syst. Sci.
Discussion started: 18 April 2019

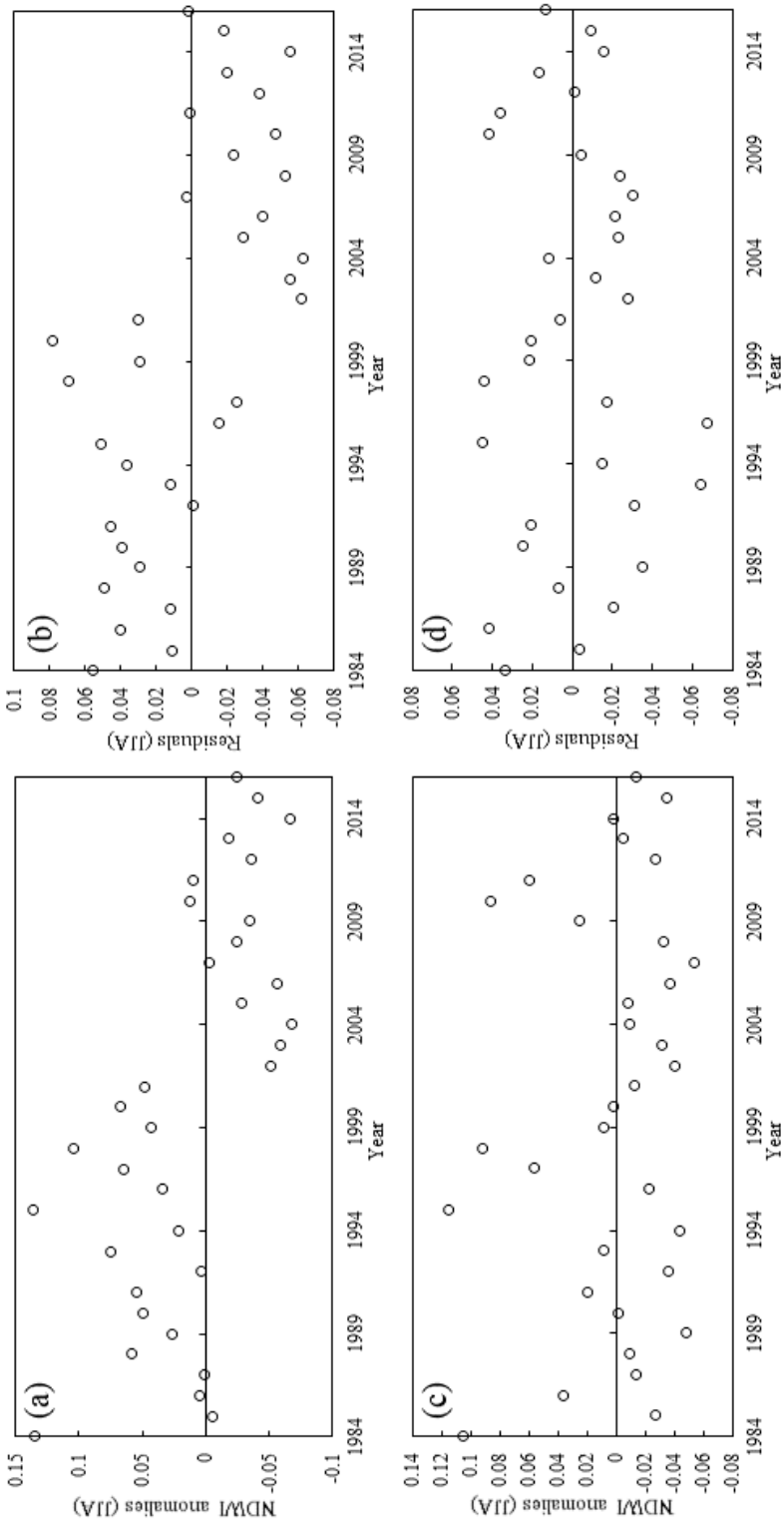

Figure 9. The Beaverhead River (BVHR4) (a) NDWI anomalies over time, (b) NDWI anomalies-climate regression residuals over time, and the Beaverhead River (BVHR2), (c) NDWI anomalies over time, (d) NDWI anomalies-climate regression residuals over time. The MK test for trends was significant (p<0.05) for (a) and (b), but not significant for (c) and (d). JJA: June, July, August.

Hydrol. Earth Syst. Sci. Discuss., https://doi.org/10.5194/hess-2019-137
Manuscript under review for journal Hydrol. Earth Syst. Sci.
Discussion started: 18 April 2019

Table 6. The per reach abundance of irrigated agriculture (Ag) at the two ends of the time period considered (1985/86 and 2016/17). Irrigation method was identified as center pivot agriculture or non-center pivot agriculture based on field shape. Accumulated ag is defined as the summed area of agriculture across the total contributing area of each reach (e.g., GR1 = agriculture area in GR1, GR2 and EGR). Riparian reaches that showed a significant non-climate related drying over time are shaded gray. Using the Mann-Whitney-Wilcoxon test, the change in fraction center pivot agriculture was significant at the $p<0.1$ level.

Reach Code	River	Center Pivot Ag (1985/86, ha)	Non-Center Pivot Ag (1985/86, ha)	Center Pivot Ag (2016/17, ha)	Non-Center Pivot Ag (2016/17, ha)	Change in Fraction Center Pivot Ag (%)	Accumulated Ag (1985/86, ha)	Accumulated Ag (2016/17, ha)
JR1	Jefferson River	571	2365	3444	1027	58	76045	78536
JR2	Jefferson River	539	2544	2344	1301	47	71432	71661
JR3	Jefferson River	601	2986	3093	1998	44	68349	68016
BVHR1	Beaverhead River	727	9034	5631	2226	64	37729	34673
BVHR2	Beaverhead River	196	11794	5794	4531	54	27967	26815
BVHR3	Beaverhead River	810	3254	3387	1772	46	11774	12084
BVHR4	Beaverhead River	0	1420	330	1039	24	1420	1368
RRR	Red Rock River	535	5754	2368	3189	34	6290	5557
BTDR	Black Tail Deer River	1066	3138	3351	1056	51	4204	4406
RR	Ruby River	540	10414	4852	5739	41	10953	10591
BHR1	Big Hole River	215	1780	768	1029	32	16080	17661
BHR2	Big Hole River	0	3992	1854	3789	33	14085	15865
BHR3	Big Hole River	52	3174	83	2515	2	3226	2597
BHR4	Big Hole River	0	6868	0	7624	0	6868	7624
MR1	Madison River	909	1445	2848	1020	35	9256	9451
MR2	Madison River	1282	5620	4128	1456	55	6902	5584
GR1	Gallatin River	441	1957	3438	1494	51	14386	22717
GR2	Gallatin River	221	8143	4407	8133	33	8364	12540
EGR	East Gallatin River	256	3367	2175	3071	34	3623	5245
	Total	**8961**	**89048**	**54294 (506% increase)**	**54006 (39% decrease)**		**398951**	**412991 (4% increase)**

Hydrol. Earth Syst. Sci. Discuss., https://doi.org/10.5194/hess-2019-137
Manuscript under review for journal Hydrol. Earth Syst. Sci.
Discussion started: 18 April 2019

584 **Table 7.** Characteristics of riparian reach contributing areas including median water table depth (m), median bedrock depth (m),
585 percent well-drained (or very well drained) soil, percent poorly (or very poorly) drained soil, elevation coefficient of variation (CV),
586 and Melton Ruggedness number. The Mann-Whitney-Wilcoxon test was used to calculate a measure of the difference (or lack of)
587 between riparian reaches that showed a significant non-climate related drying over time (shaded gray), and riparian reaches that
588 showed no such pattern, with two asterisks indicating a significant difference (p<0.05) between the two groups.

Reach Code	River	Water Table Depth (median)	Bed Rock Depth (median)	Well Drained (%)	Poorly Drained (%)	Elevation CV	Melton Ruggedness Number
JR1	Jefferson River	84	46	92	3	20	2.0
JR2	Jefferson River	54	41	87	4	13	3.0
JR3	Jefferson River	54	36	89	2	22	1.4
BVHR1	Beaverhead River	54	41	91	3	12	3.5
BVHR2	Beaverhead River	61	41	81	6	7	2.3
BVHR3	Beaverhead River	45	46	92	2	15	3.0
BVHR4	Beaverhead River	80	46	96	2	10	3.4
RRR	Red Rock River	15	46	90	4	13	1.2
BTDR	Black Tail Deer River	84	46	91	1	17	3.7
RR	Ruby River	54	48	93	3	20	1.9
BHR1	Big Hole River	54	41	99	0	10	3.1
BHR2	Big Hole River	31	41	93	2	18	1.0
BHR3	Big Hole River	15	38	91	4	13	0.8
BHR4	Big Hole River	15	40	86	5	10	1.0
MR1	Madison River	46	48	92	4	16	2.2
MR2	Madison River	54	64	60	2	15	0.3
GR1	Gallatin River	46	41	92	3	11	3.0
GR2	Gallatin River	84	48	84	3	24	1.3
EGR	East Gallatin River	84	41	83	3	21	1.3
Mann-Whitney-Wilcoxon p-value		0.45	0.37	0.04**	0.21	0.51	0.02**

589

Hydrology and Earth System Sciences
Discussions
Open Access
EGU

Hydrol. Earth Syst. Sci. Discuss., https://doi.org/10.5194/hess-2019-137
Manuscript under review for journal Hydrol. Earth Syst. Sci.
Discussion started: 18 April 2019

3.3 Trends in River Discharge

Growing-season riparian NDWI was significantly correlated (p<0.05) with growing-season river discharge at all seven USGS stream gages analyzed (Spearman correlation coefficient ranged between 0.55 along Beaverhead River and Big Hole River and 0.82 along the Jefferson River) (Table 5). In addition, all gages, except the Beaverhead River at Twin Bridges gage, were significantly correlated with spring snowfall (Spearman p-value <0.05), the climate variable that showed the highest correlation on average between summer discharge and the climate variables considered in the analysis. Unlike the riparian reaches, we saw no temporal trend (1984-2016) in the growing-season river discharge for any of the seven gages evaluated. However, because the watershed is a snowmelt-driven system, we also tested if trends were restricted to the low-flow seasons (autumn and winter). During the autumn months (September, October, November) we observed a decline in river discharge at the Madison River (p<0.05) and Gallatin River (p<0.1) gages and an increase at the Big Hole River gage near Wisdom (p<0.05), which is near the upstream end of the Big Hole River (Table 5). During the winter months (December, January, February) we observed a decline in river discharge at the Madison river gage (p<0.05) and an increase in river discharge at the Beaverhead River near the Twin Bridges gage (p<0.1) (Table 5).

4. Discussion

Across the western U.S., water withdrawals, diversions and impoundments associated with agriculture have contributed to riparian degradation (Goodwin et al., 1997; Klemas, 2014). In examining the multi-decadal trends in riparian wetness for a total of 158 km^2 of riparian ecosystem across the UMH Basin, we found long-term, significant drying along 8 of the 19 riparian reaches in this basin, including all three of the riparian reaches (the Jefferson, Madison and Gallatin Rivers) at the confluence forming the Missouri River. In contrast, we did not observe trends in growing-season river discharge or climate variables over the same period. The persistence of drying trends in riparian vegetation after accounting for the influence of climate variability, and the correlation of riparian drying with a basin-wide shift in agricultural irrigation practices, suggest that the complexities of agricultural water use and crop management are likely to be contributing factors to the drying of riparian areas in this basin. Water withdrawals across the basin are almost entirely surface-water (99%) and for irrigation (99%) (USGS 1988; Dieter et

al., 2018). The agricultural data generated in this study indicate that the basin has experienced a substantial shift from non-center pivot irrigation (e.g., gravity-fed or sprinkler) to center pivot irrigation (from 9% to 50% center pivot irrigation, basin wide). This shift in irrigation practices is concentrated along the Beaverhead, Jefferson and Gallatin Rivers, all of which showed statistically significant drying in at least portions of their riparian reaches. Correspondingly, the Big Hole River sub-watershed, which is dominated by gravity-fed irrigated hay and pasture (Montana DNRC, 2014), showed the least amount of conversion to center pivot irrigation relative to other sub-watersheds over the study period, with no temporal trends in riparian wetness.

Similar shifts in irrigation methods have occurred across the western U.S., where the percentage of agricultural land irrigated by sprinkler systems, including center pivot irrigation, increased from 28% to 59% between 1984 and 2013 (Schaible, 2017). Advances in irrigation technology allow for water to be applied at the most appropriate timing in plant root zones to increase crop consumptive use of water and therefore, crop yields (Falkenmark and Lannerstad, 2005; Ward and Pulido-Velazquez, 2008). However, despite the shift to more efficient irrigation methods, the total water-use for irrigation across the U.S. remained largely stable over the same period (Schaible, 2017). This patterns may indicate that local water savings do not necessarily translate to the watershed scale. Increases in crop yields are linearly correlated with increases in evapotranspiration (Steduto et al., 2012), so that the reduction in water application is often off-set by increases in evapotranspiration, specifically crop transpiration (Ward and Pulido-Velazquez, 2008; Grafton et al., 2018). A schematic of the potential impact of irrigation method on water cycling is shown in Fig. 10. Further, proposed water savings in per field water applications often fail to account for farm-level decisions and incentives (Ward and Pulido-Velazquez, 2008). Within the current water rights framework, more efficient water use can incentivize farmers to make changes to crop choices and crop rotation patterns, or to increase the total area irrigated or the frequency of irrigation so that their water rights and usage are maintained and maximized (Pfeiffer and Lin, 2014; Grafton et al., 2018). If there is a local reduction in water usage downstream water users can more fully exercise their water rights so that there is no net reduction in water usage at the watershed scale (Ward and Pulido-Velazquez, 2008).

651 Riparian and river condition for a given reach can be expected to be a function of its
652 upstream river network, including water added and removed from upstream reaches, as well as
653 upstream land uses (Ver Hoef and Peterson, 2012; Fritz et al., 2018). Biotic integrity, for
654 example, has been shown to depend on upstream conditions (Schofield et al., 2018), which can
655 extend tens of kilometers up the channel network (Van Sickle and Johnson, 2008). In
656 consideration of this, the climate variables used to model temporal variability in riparian wetness
657 were calculated as a function of each reach's total upstream contributing area. Additionally, we
658 considered upstream accumulated changes, such as the upstream accumulated agriculture, to help
659 interpret trends in the NDWI anomaly-climate regression residuals. Cumulative effects of both
660 climate and land use may explain why the basin's three most downstream riparian reaches (on
661 the Gallatin River, Madison River, and Jefferson River) all saw significant drying trends in the
662 NDWI anomaly-climate residuals, or the NDWI anomalies after accounting for climate
663 variability. The incremental drying effect might also help explain why we did not observe
664 temporal trends in riparian wetness in some headwater riparian reaches. For instance, along the
665 headwater riparian reaches of the Madison River (MR2), the Gallatin River (GR2), as well as the
666 East Gallatin River (EGR), the analyzed riparian vegetation extended to the upstream end of
667 irrigated agriculture. Although the total amount of agriculture varies among these riparian
668 reaches, potentially the incremental drying effects of irrigation on groundwater storage and
669 return flow do not become evident (spectrally or hydrologically) until accumulated lower in the
670 watershed. In addition to water use, landscape characteristics can inform how a riparian
671 ecosystem responds to changes in reach- or basin-scale hydrology. Well-drained soils and a
672 higher Melton Ruggedness number, characteristics significantly associated with the reach-scale
673 riparian drying trends, can be expected to facilitate the return flow of excess irrigation water to
674 the riparian corridor. Implying that a shift towards more "water efficient" irrigation might have a
675 greater drying effect on nearby riparian vegetation.
676 While the presence of riparian drying trends in the NDWI anomaly-climate residuals
677 indicated that the observed drying trends were not solely attributable to climate, climate
678 variability was a significant predictor of the interannual variability in riparian wetness (e.g., Fig.
679 5 and Fig. 6), a finding documented in other geographic regions as well (e.g., Fu and Burgher,
680 2015; Nguyen et al., 2015; Huntington et al., 2016). Drought events, and the resilience of river
681 and riparian ecosystems to these events, are a significant concern for stakeholders in the Upper

682 Missouri Headwaters Basin (Montana DNRC, 2015; McEvoy et al., 2018). Although evaluation
683 of water rights and corresponding water withdrawals under drought conditions was beyond the
684 scope of this study, our findings suggest that the conversion to center pivot irrigation could
685 amplify the impacts of reduced precipitation on riparian areas. Additionally, an increasing
686 summer VPD could further increase crop water losses to evapotranspiration (Massmann et al.,
687 2018), potentially exacerbating both the hydrological effect and salinization effect of irrigation
688 conversion (Singh, 2015). We note, however, that climate and river discharge trends were
689 quantified only to be compared with trends observed in riparian wetness over the same period
690 (1984-2016). Because only partial climate and river discharge records were used, our findings
691 regarding the presence or absence of trends in the climate and river discharge data should be
692 interpreted with caution.
693 Despite only partial discharge records being utilized, one interesting finding was that
694 over the same period a drying trend in riparian areas did not necessarily translate into a trend in
695 river discharge. We can speculate that because the rivers are snow-melt dominated (Markstrom
696 et al., 2016; Cross et al., 2017), during the summer months irrigation return flow may have an
697 impact on riparian areas but could represent a relatively small percent of summer flows. A
698 comprehensive water budget or hydrological modeling approach, however, would be needed to
699 quantify this, and specifically to determine how anthropogenic activities may have a differential
700 impact on riparian wetness relative to river discharge. Additionally, rivers across the basin vary
701 in the amount of flow regulation from dams. For example, the Big Hole River and Gallatin
702 Rivers are relatively unregulated while the Madison River, Beaverhead River, Ruby River and
703 Red Rock River are all regulated by dams. The reservoirs above dams retain water during the
704 spring runoff, reducing peak flows, and release more water in the autumn, changing a river's
705 natural flow regime (Montana DNRC, 2014). It is possible that shifts in dam management and
706 corresponding changes in flow regulation could contribute to trends in riparian wetness.
707 However, river discharge (JJA) was significantly correlated with spring snowfall at eight of nine
708 gages, suggesting that even with seasonal flow regulation, discharge along dammed rivers still
709 typically represents interannual variability in climate.
710 Efforts to characterize the factors influencing variability and trends in riparian wetness
711 are critical to maintain and restore riparian functionality. Healthy floodplains and riparian areas
712 serve a number of functions including slowing runoff, promoting local groundwater recharge,

713 and quickening the recovery of local groundwater storage post-drought (Montana DNRC, 2014).
714 Spectral indices calculated from satellite imagery have been successfully used to monitor the
715 response of riparian vegetation to variability in channel morphology (Henshaw et al., 2013;
716 Hamdan and Myint, 2015), as well as changes induced by the installation of in-stream restoration
717 structures (Hausner et al. 2018; Vanderhoof and Burt, 2018). While Landsat has been commonly
718 used to examine multi-decadal trends in vegetation condition (Goetz et al., 2005; McManus et
719 al., 2012; White et al., 2017), because of the narrow, linear footprint of riparian ecosystems
720 within human-influenced landscapes, efforts to apply Landsat time-series analysis to riparian
721 systems have been limited (e.g., Henshaw et al., 2013; Hamden and Myint, 2015; Nguyen et al.,
722 2015). Regional-scale Landsat efforts have tended to focus on changes to riparian extent rather
723 than riparian trends in greenness or wetness (e.g., Jones et al., 2010; Macfarlane et al., 2017).
724 Along river systems, however, the moderate resolution of Landsat can misrepresent riparian
725 edges or fail to detect portions of the riparian corridor that are narrower than Landsat's minimum
726 mapping unit, potentially influencing the calculated spectral patterns. In our analysis we
727 minimized such errors by (1) restricting the analysis to rivers with riparian corridors large
728 enough to be measured using Landsat, and (2) using a consistent riparian area extent across the
729 time series. It is clear, however, that finer spatial resolution sources of imagery will be critical
730 for riparian corridors too narrow to be monitored with Landsat imagery. To this end, data sources
731 with increased spatial resolution are rapidly becoming more available and useful for monitoring
732 water resources (e.g., Sentinel-2, CubeSats) (e.g., Vande Kamp et al., 2013; Gärtner et al., 2016;
733 Cooley et al., 2017; Yang et al., 2017), but lack the multi-decadal data records provided by
734 Landsat. This means that for larger riparian corridors, Landsat spectral indices remain a critical
735 data source that can be used to characterize trends in riparian wetness as well as potentially
736 quantify the impact of land use changes, including long-term shifts in irrigation methods, on
737 riparian vegetation.
738

Hydrol. Earth Syst. Sci. Discuss., https://doi.org/10.5194/hess-2019-137
Manuscript under review for journal Hydrol. Earth Syst. Sci.
Discussion started: 18 April 2019

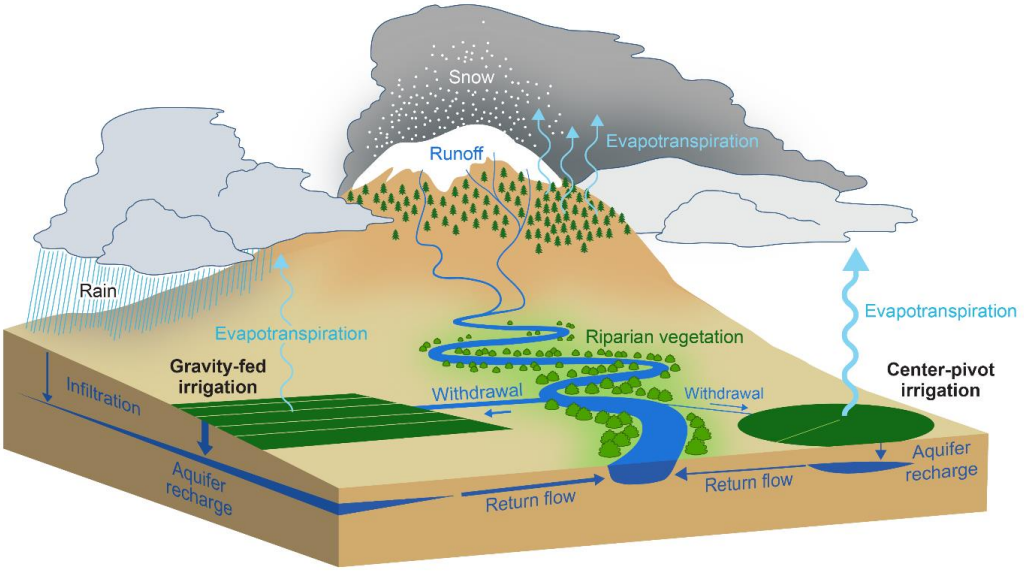

Figure 10. A schematic showing the potential impacts of changing irrigation types. While shifting to center-pivot irrigation can be expected to reduce per-field water applications, it can also be expected to increase evapotranspiration as well as decrease sub-surface return-flow and aquifer recharge. Reduced withdrawal may not persist downstream but instead be used by the same farmer or a downstream user. Thicker and thinner lines are used to indicate more or less water, respectively.

5. Conclusion

Riparian corridors provide valuable ecosystem functions including storing water, nutrients, pollutants, and sediments, providing wildlife corridors, and influencing water temperature (Vivoni et al., 2006; Lees and Peres, 2008; Isaak et al., 2012). A drying trend in riparian areas across the Upper Missouri Headwaters Basin could lessen the effectiveness of these functions and shift the systems towards more drought-tolerant plant species that are less adapted to highly variable flow regimes (Capon, 2013; Catford et al., 2014). Although promoted as a more water-efficient approach, several recent studies have demonstrated a lack of catchment-scale water savings after farmers shift towards center pivot irrigation (Perry, 2017; Grafton et al., 2018). We were able to pair a Landsat time series analysis with climate and agricultural data to document a statistically significant drying trend, not explained by climate variability, along nearly half (42%) of riparian reaches in the Upper Missouri Headwaters Basin. Although the riparian reaches experiencing drying trends tended to have more upstream agriculture and greater shifts toward center pivot irrigation, the correlations between agricultural

activities and riparian wetness were imperfect, suggesting that the upstream river network, as well as other reach-scale characteristics such as the riparian species or the geology/soil characteristics, also influence the response of a riparian reach to changes in water withdrawal. In addition, the drying trends in riparian ecosystems were not observed in the snow-melt driven river discharge (JJA), a finding that should be explored further using hydrological models. Maintaining and improving riparian functionality across watersheds dominated by agricultural activity will require not only more efforts to track temporal trends in riparian vegetation, but also more efforts to separate out the relative influence of climate and anthropogenic activities.

6. Acknowledgements

This project was funded by the U.S. Geological Survey, Land Resources, Land Change Science Program as well as by a U.S. EPA Region 8 grant, entitled “Building drought resiliency and watershed prioritization using natural water storage techniques” and through the associated interagency agreement (DW-014-92475401-0). We thank Haley Distler for her assistance in delineating the riparian corridor and Jeremey Havens for his assistance in generating the hydrology schematic. We also thank Ken Fritz and Robert Payn for their insightful comments on earlier versions of this manuscript. Following publication, the data related to this publication will be published in the U.S. Geological Survey’s ScienceBase catalog (https://doi.org/10.5066/P976LZ2G). Any use of trade, firm, or product names is for descriptive purposes only and does not imply endorsement by the U.S. Government. This publication represents the views of the authors and does not necessarily reflect the views or policies of the U.S. EPA.

7. Author Contributions: MV, JC, and LA designed the study, MV and JC derived the input datasets, MV performed the analysis, and MV, JC, and LA wrote the manuscript.

8. Competing interests: The authors declare that they have no conflict of interest.

9. References

790 Ascione, A., Cinque, A., Miccadei, E., Villani, F., Berti, C.: The Plio-Quaternary uplift
791 of the Apennine chain: New data from the analysis of topography and river valleys in
792 Central Italy, Geomorphology, 102, 105-118, 2008.
793 Bauder, J. W.: Early season alfalfa irrigation strategies. Montana State University Extension,
794 Bozeman, MT. Available at http://waterquality.montana.edu/farm-
795 ranch/irrigation/alfalfa/early.html (last accessed, November 19, 2018), 2018.
796 Boutin, C., Belanger, J.B.: Importance of riparian habitats to flora conservation in farming
797 landscapes of southern Quebec, Canada, Agr. Ecosyst. Environ., 94, 73–87, 2003.
798 Carrillo-Guerrero, Y., Glenn, E. P., Hinojosa-Huerta, O.: Water budget for agricultural and
799 aquatic ecosystems in the delta of the Colorado River, Mexico: Implications for obtaining
800 water for the environment, Ecol. Eng., 59, 41-51, 2013.
801 Catford, J. A., Morris, W. K., Vesk, P. A., Gippel, C. J., Downes, B. J.: Species and
802 environmental characteristics point to flow regulation and drought as drivers of riparian
803 plant invasion, Biodiv. Res., 20(9), 1084-1096, 2014.
804 Chatterjee, C., Kumar, R., Chakravorty, B., Lohani, A. K., Kumar, S.: Integrating remote
805 sensing and GIS techniques with groundwater flow modeling for assessment of
806 waterlogged areas, Water Resour. Manag., 19(5), 539-554, 2005.
807 Chowdary, V. M., Vinu Chandran, R., Neeti, N., Bothale, R. V., Srivastava, Y. K., Ingle, P.,
808 Ramakrishnan, D., Dutta, D., Jeyaram, A., Sharma, J.R., Singh, R.: Assessment of surface
809 and sub-surface waterlogged areas in irrigation command areas of Bihar state using remote
810 sensing and GIS, Agr. Water Manag., 95, 754–766, 2008.
811 Clancy, C. G.: Effects of dewatering on spawning by Yellowstone cutthroat trout in tributaries of
812 the Yellowstone River, Montana, Am. Fish. Soc. Symp., 4, 37-41, 1988.
813 Clifford, M.: Preserving stream flows in Montana through the Constitutional Public Trust
814 Doctrine: An underrated solution, Publ. Land Law Rev., 16, 117-135, 1995.
815 Cohen, J.: Statistical Power Analysis for the Behavioral Sciences, 2nd Edition. Routledge, 1988.
816 Cooley, S., Smith, L., Stepan, L., Mascaro, J. Tracking dynamic northern surface water changes
817 with high-frequency Planet CubeSat imagery, Rem. Sens., 9, 1306, 2017.
818 Crétaux, J.-F., Biancamaria, S., Arsen, A., Bergé-Nguyen, M., Becker, M.: Global surveys of
819 reservoirs and lakes from satellites and regional application to the Syrdarya river
820 basin, Environ. Res. Lett., 10, 015002, 2015.

821 Cross, W. F., LaFave, J., Leone, A., Lonsdale, W., Royem, A., Patton, T., McGinnis, S.: Chapter
822 3, Water and climate change in Montana, in the 2017 Montana Climate Assessment (ed. C.
823 Whitlock, W. F. Cross, B. Maxwell, N. Silverman, A. A. Wade), Helena, MT, 77 pgs, 2017.
824 Cunningham, S. C., Thomson, J. R., Mac Nally, R., Read, J., Baker, P. J.: Groundwater change
825 forecasts widespread forest dieback across an extensive floodplain system, Freshwat. Biol.,
826 56, 1494-1508, 2011.
827 Dieter, C. A., Linsey, K. S., Caldwell, R. R., Harris, M. A., Ivahnenko, T. I., Lovelace, J. K.,
828 Maupin, M. A., Barber, N. L. Estimated use of water in the United States county-level data
829 for 2015. U.S. Geological Survey, Reston, VA, 2018.
830 Dragoni, W., Sukhiga, B. S.: Climate change and groundwater: a short review. Geol Soc Lond
831 Spec Publ, 288, 1–12, 2008.
832 Duffield, J., Neher, C. J., Brown, T. C.: Recreation benefits of instream flow: Application to
833 Montana Big Hole and Bitterroot Rivers, Water Resour. Res., 28, 2169-2181, 1992.
834 Falkenmark, M., Lannerstad, M.: Consumptive water use to feed humanity – curing a blind spot,
835 Hydrol. Earth Syst. Sci., 9, 15– 28, doi:10.5194/hess-9-15-2005, 2005
836 Fritz, K. M., Schofield, K. A., Alexander, L. C., McManus, M. G., Golden, H. E., Lane, C. R.,
837 Kepner, W. G., LeDuc, S. D., DeMeester, J. E., Pollard, A. I.: Physical and chemical
838 connectivity of streams and riparian wetlands to downstream waters: a synthesis. J. Am.
839 Water Res. Assoc., 54(2), 323-345, 2018.
840 Fu, B., Burgher, I.: Riparian vegetation NDVI dynamics and its relationship with climate,
841 surface water and groundwater. J. Arid Environ., 113, 59-68, 2015.
842 Gao, B.: NDWI—a normalized difference water index for remote sensing of vegetation liquid
843 water from space. Rem. Sens. Environ., 58, 257 – 266, 1996.
844 Gärtner, P., Förster, M., Kleinschmit, B.: The benefit of synthetically generated RapidEye and
845 Landsat 8 data fusion time series for riparian forest disturbance monitoring. Rem. Sens.
846 Environ., 177, 237-247, 2016.
847 Gesch, D., Oimoen, M., Greenlee, S., Nelson, C., Steuck, M., Tyler, D. The National Elevation
848 Dataset. Photogramm. Eng. Rem. Sens., 68(1), 5–11, 2002.
849 Gilbert, R. O.: Statistical Methods for Environmental Pollution Monitoring, Wiley, NY, 1987.

850 Goetz, S. J., Bunn, A. G., Fiske, G. J., Houghton, R. A.: Satellite-observed photosynthetic trends
851 across boreal North America associated with climate and fire disturbance, Proc. Natl. Acad.
852 Sci. Unit. States Am., 102(38), 13521-13525, 2005.
853 Goklany, I. M.: Comparing 20th century trends in U.S. and global agricultural water and land
854 use, Water Int., 27, 321–329, 2002.
855 Goodwin, C. N., Hawkins, C. P., Kershner J. L.: Riparian restoration in the western United
856 States: overview and perspective, Restor. Ecol., 5, 4-14, 1997.
857 Goudie A. S.: Global warming and fluvial geomorphology, Geomorphology, 79, 384–94, 2006.
858 Gosnell, H., Haggerty, J. H., Byorth, P. A. Ranch ownership change and new approaches to
859 water resource management in southwestern Montana: implications for fisheries. J. Am.
860 Water Res. Assoc., 43(4), 990-1003, 2007.
861 Grafton, R. Q., Williams, J., Perry, C. J., Molle, F., Ringler, C., Steduto, P., Udall, B., Wheeler,
862 S. A., Wang, Y., Garrick, D., Allen, R. G. The paradox of irrigation efficiency, Science,
863 361(6404), 748-750, 2018.
864 Gude, P. H., Hansen, A. J., Rasker, R., Maxwell, B.: Rates and drivers of rural residential
865 development in the Greater Yellowstone, Landsc. Urban Plan., 77, 131–151, 2006.
866 Hackett, O. M., Visher, F. N., McMurtrey, R. G., and Steinhilber, W. L.: Geology and ground
867 water resources of the Gallatin Valley, Gallatin County, Montana, U.S. Geological Survey
868 Water-Supply Paper 1482, 282, 1960.
869 Hamdan, A., Myint, S. W.: Biogeomorphic relationships and riparian vegetation changes along
870 altered ephemeral stream channels: Florence to Marana, Arizona, Prof. Geogr., 68(1), 26-38,
871 2015.
872 Hamed, K. H., Rao, A. R.: A modified Mann-Kendall trend test for autocorrelated data. J.
873 Hydrol., 2014(1-4), 182-196, 1998.
874 Hansen, A. J., Rasker, R., Maxwell, B., Rotella, J. J., Johnson, J. D., Parmenter, A. W., Langner,
875 U., Cohen, W. B., Lawrence, R. L., Kraska, P. V.: Ecological causes and consequences of
876 demographic change in the new west, Bioscience, 52, 151–162, 2002.
877 Hastie, T., Tibshirani, R., Friedman, J. The Elements of Statistical Learning. New York:
878 Springer, 2009.
879 Hausner, M. B., Huntington, J. L., Nash, C., Morton, C., McEvoy, D. J., Pilliod, D. S.,
880 Hegewisch, K. C., Daudert, B., Abatzoglou, J. T., Grant, G.: Assessing the effectiveness of

riparian restoration projects using Landsat and precipitation data from the cloud-computing application ClimateEngine.org, Ecolog. Eng., 120, 432-440, 2018.

Henshaw, A. J., Gurnell, A. M., Bertoldi, W., Drake, N. A.: An assessment of the degree to which Landsat TM data can support the assessment of fluvial dynamics, as revealed by changes in vegetation extent and channel position, along a large river, Geomorphology, 202, 74-85, 2013.

Homer, C., Dewitx, J., Yang, L., Jin, S., Danielson, P., Xian, G., Coulston, J., Herold, N., Wickham, J., Megown, K.: Completion of the 2011 National Land Cover Database for the conterminous United States—Representing a decade of land cover change information, Photogramm. Eng. Rem. Sens., 81, 345–354, 2015.

Huntington, J., McGwire, K., Morton, C., Snyder, K., Peterson, S., Erckson, T., Niswonger, R., Carroll, R., Smith, G., Allen, R.: Assessing the role of climate and resource management on groundwater dependent ecosystem changes in arid environments with the Landsat archive. Rem. Sens. Environ., 185, 186-197, 2016.

Hurvich, C.M., Tsai, C.L.: Regression and time series model selection in small samples, Biometrika, 76(2), 297-307, 1989.

Isaak, D. J., Wollrab, S., Horan, D., Chandler, G.: Climate change effects on stream and river temperatures across the northwest U.S. from 1980-2009 and implications for salmonid fishes, Climatic Change, 113(2), 499-524, 2012.

Jones, H. P., Hole, D. G., Zavaleta, E. S.: Harnessing nature to help people adapt to climate change, Nat. Clim. Chang., 2, 504–509, 2012.

Jones, K. B., Edmonds, C. E., Slonecker, E. T., Wickham, J. D., Neale, A. C., Wade, T. G., Riiters, K.H., Kepner, W.G.: Detecting changes in riparian habitat conditions based on patterns of greenness change: A case study from the Upper San Pedro River Basin, USA, Ecol. Indic., 8, 89–99, 2008.

Jones, K. B., Slonecker, E. T., Nash, M. S., Neale, A. C., Wade, T. G., Hamann, S.: Riparian habitat changes across the continental United States (1972-2003) and potential implications for sustaining ecosystem services, Landsc. Ecol., 25, 1261-1275, 2010.

Kendall, M. G.: Rank Correlation Methods, Griffin, London, 1975.

Kendy, E., Bredehoeft, J. D.: Transient effects of groundwater pumping and surface-water irrigation returns on streamflow, Water Resour. Res., 42, W08415, 2006.

912 Kerkvliet, J., Nowell, C., Lowe, S. The economic value of the Greater Yellowstone's Blue-
913 Ribbon fishery, N. Am. J. Fish. Manag., 22, 418-424, 2002.
914 Klemas, V.: Remote sensing of riparian and wetland buffers: an overview. J. Coast.
915 Res., 30, 869-880, 2014.
916 Lees, A. C., Peres, C. A.: Conservation value of remnant riparian forests corridors of varying
917 quality for amazonian birds and mammals. Conserv. Biol., 2, 439-449, 2008.
918 Leyk, S. Uhl, J. H.: Historical built-up intensity layer series for the U.S. 1810 -
919 2015, https://doi.org/10.7910/DVN/1WB9E4, Harvard Dataverse, V1, 2018.
920 Liaw, A., Wiener, M.: Breiman and Cutler's random forests for classification and regression; R
921 package version 4.6-12; R Foundation for Statistical Computing: Vienna, Austria, 1-29,
922 2015.
923 Lowrance, R., Todd, R., Fail Jr., J., Hendrickson Jr., O., Leonard, R., Asmussen, L.: Riparian
924 forests as nutrient filters in agricultural watersheds, Bioscience, 34, 374–377, 1984.
925 Macfarlane, W. W., Gilbert, J. T., Jensen, M. L., Gilbert, J. D., Hough-Snee, N., McHugh, P. A.,
926 Wheaton, J. M., Bennett, S. N. Riparian vegetation as an indicator of riparian condition:
927 detecting departures from historic condition across the North American West. J. Environ.
928 Manag., 202(part 2), 447-460, 2017.
929 Mann, H. B.: Nonparametric tests against trend, Econometrica, 13, 245-259, 1945.
930 Markstrom, S. L., Hay, L. E., Clark, M. P. Towards simplification of hydrologic modeling:
931 identification of dominant processes, Hydrol. Earth Syst. Sci., 20, 4655-4671, 2016.
932 Massmann, A., Gentine, P., Lin, C.: When does vapor pressure deficit drive or reduce
933 evapotranspiration?, Hydrol. Earth Syst. Sci. Discuss., https://doi.org/10.5194/hess-2018-
934 553, in review, 2018.
935 McEvoy, J., Bathke, D. J., Burkardt, N., Cravens, A. E., Haigh, T., Hall, K. R., Hayes, M. J.,
936 Jedd, T., Podebradska, M., Wickham, E.: Ecological drought: Accounting for the non-
937 human impacts of water shortage in the Upper Missouri Headwaters Basin, Montana, USA,
938 Resources, 7(14), 1-17, 2018.
939 McFeeters, S. K.: The use of normalized difference water index (NDWI) in the delineation of
940 open water features, Internat. J. Rem. Sens., 17: 1425–1432, 1996.

941 McFeeters, S. K.: Using the Normalized Difference Water Index within a geographic
942 information system to detect swimming pools for mosquito abatement: a practical approach,
943 Rem. Sens., 5(7), 3544-3561, 2013.
944 McManus, K. M., Morton, D. C., Masek, J. G., Wang, D., Sexton, J. O., Nagol, J. R., Ropars, P.,
945 Boudreau, S.: Satellite-based evidence for shrub and graminoid tundra expansion in
946 northern Quebec from 1986 to 2010, Global Change Biol., 18(7), 2313-2323, 2012.
947 Melton, M. A. The geomorphic and paleoclimatic significance of alluvial deposits in southern
948 Arizona, J. Geology, 73, 1–38, 1965.
949 Montana Department of Natural Resources and Conservation (DNRC): Upper Missouri Basin
950 Water Plan 2014, Montana Department of Natural Resources and Conservation, Helena, MT,
951 219 pgs, 2014.
952 Montana Department of Natural Resources and Conservation (DNRC): Montana State Water
953 Plan, Montana Department of Natural Resources and Conservation, Helena, MT, 64 pgs.,
954 2015.
955 Murphy, M. A., Evans, J. S., Storfer, A.: Quantifying Bufo boreas connectivity in Yellowstone
956 National Park with landscape genetics, Ecology, 91(1), 252-261, 2010.
957 Naiman, R. J., De´camps, H., McClain, M. E. Riparia: ecology, conservation and management of
958 streamside communities. New York: Academic Press, 2005.
959 National Snow and Ice Data Center (NSIDC). All about snow. National Snow and Ice Data
960 Center, Boulder, CO. (last accessed, 3 October 2018), 2018.
961 Nguyen, U., Glen, E. P., Nagler, P. L., Scott, R. L.: Long-term decrease in satellite vegetation
962 indices in response to environmental variables in an iconic desert riparian ecosystem: The
963 Upper San Pedro, Arizona, United States, Ecohydrology, 8, 610-625, 2015.
964 Nilsson, C., Berggren, K.: Alterations of riparian ecosystems caused by river regulation,
965 Bioscience, 50, 783–792, 2000.
966 NOAA National Climatic Data Center: Data Tools: 1981-2010 Normals. Available at
967 http://www.ncdc.noaa.gov/cdo-web/datatools/normals, (last accessed 3 October 2018), 2014.
968 Pederson, G. T., Betancourt, J. L., McCabe, G. J.: Regional patterns and proximal causes of the
969 60 recent snowpack decline in the Rocky Mountains, U.S., Geophys. Res. Lett., 40, 1811–
970 1816, 2013.

971 Pederson, G. T., Gray, S. T., Woodhouse, C. A., Betancourt, J. L., Fagre, D. B., Littell, J. S.,
972 Watson, E., Luckman, B. H., Graumlich, L. J.: The unusual nature of recent snowpack
973 declines in the North American Cordillera, Science, 333, 332–335, 2011.
974 Perry, C., Steduto, P., Karejeh, F.: Does improved irrigation technology save water? A review of
975 the evidence. Food and Agriculture Organization of the United Nations, Cairo, Egypt, 57
976 pgs., 2017.
977 Peterson, E. E.: STARS: Spatial Tools for the Analysis of River Systems version 2.0.6 – a
978 tutorial, Queensland University of Technology, Brisbane, Australia, 47 pgs., 2017.
979 Peterson, J. M., Ding, Y.: Economic adjustments to groundwater depletion in the high plains: Do
980 water-saving irrigation systems save water? Am. J. Agric. Econ., 87, 147–159, 2005.
981 Pfeiffer, L., Lin, C. Y. C.: Does efficient irrigation technology lead to reduced groundwater
982 extraction? Empirical evidence. J. Environ. Econ. Manag., 67(2), 189-208, 2014.
983 Poff, N. L., Allan, J. D., Bain, M. B., Karr, J. R., Prestagaard, K. L.: The natural flow regime,
984 BioScience, 47, 769-784, 1997.
985 Poff, B. Koestner, K. A. Neary, D .G. Henderson, V.: Threats to riparian ecosystems in Western
986 North America: an analysis of existing literature, J. Am. Water Resour. As, 47, 1241-1254,
987 2011.
988 Poole, G. C., Berman, C. H.: An ecological perspective on in-stream temperature: Natural heat
989 dynamics and mechanisms of human-caused thermal degradation, Environ. Manag., 27(6),
990 787-802, 2001.
991 PRISM Climate Group, Oregon State University: Available at http://prism.oregonstate.edu. (last
992 accessed on 27 June, 2018), 2018.
993 Richardson, D. M., Holmes, P. M., Esler, K. J., Galatowitsch, S. M., Stromberg, J. C., Kirkman,
994 S. P., Pysek, P., Hobbs, R. J.: Riparian vegetation: Degradation, alien plant invasions, and
995 restoration prospects, Divers. Distrib., 13, 126–139, 2007.
996 Rood, S. B., Pan, J., Gill, K. M., Franks, C. G., Samuelson, G. M., Shepherd, A: Declining
997 summer flows of Rocky Mountain rivers: changing seasonal hydrology and probable
998 impacts on floodplain forests, J. Hydrol., 349, 397–410, 2008.
999 Schaible, G.: Understanding irrigated agriculture. Statistic: Farm Practices & Management, U.S.
1000 Department of Agriculture, Economic Research Service, 6 pgs., 2017.

1001 Schaible, G .D., Aillery, M. P.: Water conservation in irrigated agriculture: Trends and
1002 challenges in the face of emerging demands, EIB-99, U.S. Department of Agriculture,
1003 Economic Research Service: Washington, DC, USA, 2012.
1004 Schofield, K. A., Alexander, L. C., Ridley, C. E., Vanderhoof, M. K., Fritz, K. M., Autrey, B.,
1005 DeMeester, J., Kepner, W. G., Lane, C. R., Leibowitz, S., Pollard, A. I.: Biota connect
1006 aquatic habitats throughout freshwater ecosystem mosaics. J. Am. Water Res. Assoc., 54(2),
1007 372-399, DOI: 10.1111/1752-1688.12634, 2018.
1008 Shafroth, P. B., Stromberg, J. C., Patten, D. T.: Riparian vegetation response to altered
1009 disturbance and stress regimes, Ecol. Applic., 12(1), 107-123, 2002.
1010 Singh, A.: Soil salinization and waterlogging: A threat to environment and agricultural
1011 sustainability, Ecol. Indic., 57, 128-130, 2015.
1012 Slagle, S. E.:Geohydrologic conditions and land use in the Gallatin Valley, southwestern
1013 Montana, 1992-93. U. S. Geological Survey Water-Resources Investigations Report 95-4034,
1014 2 p., 1995.
1015 Soil Survey Staff, Natural Resources Conservation Service, United States Department of
1016 Agriculture. Soil Survey Geographic (SSURGO) Database for [Montana]. Available online at
1017 https://sdmdataaccess.sc.egov.usda.gov. Accessed [6/25/2018].
1018 Steduto, P., Hsiao, T. C., Fereres, E., Raes, D.: Crop yield response to water. Food and
1019 Agricultural Organization, Irrigation and Drainage Paper 66, Rome, Italy, 505 pgs., 2012.
1020 Stromberg, J. C.: Restoration of riparian vegetation in the south-western United States:
1021 Importance of flow regimes and fluvial dynamism, J. Arid Environ., 49, 17–34, 2001.
1022 Stromberg, J. C., Lite, S. J., Rychener, T. J., Levick, L. R., Dixon, M. D., Watts, J. M.: Status of
1023 the riparian ecosystem in the Upper San Pedro River, Arizona: Application of an assessment
1024 model, Environ. Monit. Assess., 115, 145–173, 2006.
1025 Sweeney, B. W., Bott, T. L., Jackson, J. K., Kaplan, L. A., Newbold, J. D., Standley, L. J,
1026 Horwitz, R. J., Hession, W. C.: Riparian deforestation, stream narrowing, and loss of stream
1027 ecosystem services. Proc. Natl. Acad. Sci. Unit. States Am., 101, 14132–14137, 2004.
1028 Theobald, D. M., Norman, J. B., Peterson, E., Ferraz, S., Wade, A., Sherburne, M. R.:
1029 Functional linkage of water basins and streams (FLoWS) v1 user's guide: ArcGIS tools
1030 for network-based analysis of freshwater ecosystems. Natural Resource Ecology Lab,
1031 Colorado State University, Fort Collins, CO, 43 pgs., 2006.

1032 Tucker, C. J.: Red and photographic infrared linear combinations for monitoring
1033 vegetation, Rem. Sens. Environ., 8, 127–150, 1979.
1034 U.S. Bureau of Reclamation (USBR): Climate Change Analysis for the Missouri River Basin,
1035 Technical Memorandum No. 86-68210-2012-03, U.S. Bureau of Reclamation: Washington,
1036 DC, USA, 2012.
1037 U.S. Department of Agriculture (USDA): National Agricultural Statistics Service Cropland Data
1038 Layer [Online]. Available at https://nassgeodata.gmu.edu/CropScape/ (last accessed
1039 November 5, 2018), USDA-NASS, Washington, DC., 2018.
1040 U.S. Geological Society (USGS): U.S. Geological Survey, Water Resources of the United States
1041 [Online]. ScienceBase Data Publication
1042 (https://www.sciencebase.gov/catalog/item/57361cc8e4b0dae0d5df6d22), Reston, VA, 1988.
1043 Vanderhoof, M. K., Burt, C.: Applying high-resolution imagery to evaluate restoration-induced
1044 changes in stream condition, Missouri River Headwaters Basin, Montana, Rem. Sens., 10(6),
1045 913, DOI: 10.3390/rs10060913, 2018.
1046 Vanderhoof, M. K.: Lane, C.R.: The potential role of very high-resolution imagery to
1047 characterize lake, wetland and stream systems across the Prairie Pothole Region, United
1048 States, Intern. J. Rem. Sens., 10.1080/01431161.2019.1582112, 2019.
1049 Van Sickle, J., Johnson, C. B.: Parametric distance weighting of landscape influence on streams,
1050 Landsc. Ecol., 23(4), 427-438, 2008.
1051 Vande Kamp, K., Rigge, M., Troelstrup, Jr., N.H., Smart, A.J., Wylie, B.: Detecting channel
1052 riparian vegetation response to best-management-practices implementation in ephemeral
1053 streams with the use of Spot high-resolution visible imagery, Rang. Ecol. Manage., 66, 63-
1054 70, 2013.
1055 Ver Hoef, J. M., Peterson, E. E.: A moving average approach for spatial statistical models of
1056 stream networks, J. Am. Stat. Assoc., 105, 489, 6-18, 2012.
1057 Vivoni, E., Bowman, R. S., Wychkoff, R. L., Jakubowski, R. T., Richards, K. E.: Analysis of a
1058 monsoon flood event in an ephemeral tributary and its downstream hydrologic effects, Water
1059 Resour. Res., 42(3), W03404, 2006.
1060 Ward, F. A., Pulido-Velazquez, M.: Water conservation in irrigation can increase water use,
1061 Proc. Natl. Acad. Sci. Unit. States Am., 105(47), 18215-18220, 2008.

White, J. C., Wulder, M. A., Hermosilla, T., Coops, N. C., Hobart, G. W.: Nationwide annual characterization of 25 years of forest disturbance and recovery for Canada using Landsat time series, Rem. Sens. Environ., 194, 303-321, 2017.

Wisser, D., Frolking, S., Douglas, E. M., Fekete, B. M., Vörösmarty, C. J., Schumann, A. H.: Global irrigation water demand: variability and uncertainties arising from agricultural and climate data sets. Geophys. Res. Lett., 35(24), 1-5, 2008.

Yang, X., Zhao, S., Qin, X., Zhao, N., Liang, L.: Mapping of urban surface water bodies from Sentinel-2 MSI imagery at 10 m resolution via NDWI-based image sharpening. Remot. Sens., 9(6), 596, 2017.

Ziemer, L. S., Kendy, E., Wilson, J.: Ground water management in Montana: On the road from beleaguered to science-based policy, Publ. Land Resour. Law Rev., 76, 75–97, 2006.